

**Modified Reverse Osmosis System
for Treatment of Produced Waters**

Annual Technical Progress Report

Reporting Period: September 14, 2001–September 15, 2002

Principal Author: T. M. Whitworth
(573) 485-2276

Secondary Authors: Liangxiong Li

Report Date: September 15, 2002

DOE Award Number: DE-FC-26-00-BC15326

Name and Address
of Submitting Organization:
Petroleum Recovery Research Center
New Mexico Tech
801 Leroy Place
Socorro, New Mexico 87801

NM PRRC Contributors:
Robert Lee, Tianguang Fan, Jeremiah Wright,
Bing Ye, Eric Garlinger, and Jonathan Fischer

DISCLAIMER

This report was prepared as an account of work sponsored by an agency of the United States Government. Neither the United States Government nor any agency thereof, nor any of their employees, make any warranty, expressed or implied, or assumes any legal liability or responsibility for the accuracy, completeness, or usefulness of any information, apparatus, product, or process disclosed, or represents that its use would not infringe on privately owned rights. Reference herein to any specific commercial product, process, or service by trade name, trademark, manufacturer, or otherwise does not necessarily constitute or imply its endorsement, recommendation, or favoring by the United States Government or any agency thereof. The views and opinions of authors expressed herein do not necessarily state or reflect those of the United States Government.

ABSTRACT

This report describes work performed during the first year of the project “Modified Reverse Osmosis System for Treatment of Produced Waters.” This research project has two objectives. The first objective is to test the use of clay membranes in the treatment of produced waters by reverse osmosis. The second objective is to test the ability of a system patented by the New Mexico Tech Research Foundation to remove salts from reverse osmosis waste streams as a solid. We performed 12 experiments using clay membranes in cross-flow experimental cells. We found that, due to dispersion in the porous frit used adjacent to the membrane, the concentration polarization layer seems to be completely (or nearly completely) destroyed at low flow rates. This observation suggests that clay membranes used with porous frit material may reach optimum rejection rates at lower pumping rates than required for use with synthetic membranes. The solute rejection efficiency decreases with increasing solution concentration. For the membranes and experiments reported here, the rejection efficiency ranged from 71% with 0.01 M NaCl solution down to 12 % with 2.3 M NaCl solution. More compacted clay membranes will have higher rejection capabilities. The clay membranes used in our experiments were relatively thick (approximately 0.5 mm). The active layer of most synthetic membranes is only 0.04 μm (0.00004 mm), approximately 1250 times thinner than the clay membranes used in these experiments. Yet clay membranes as thin as 12 μm have been constructed (Fritz and Eady, 1985). Since Darcy’s law states that the flow through a material of constant permeability is inversely proportional to its material’s thickness, then, based on these experimental observations, a very thin clay membrane would be expected to have much higher flow rates than the ones used in these experiments. Future experiments will focus on testing very thin clay membranes. The membranes generally exhibited reasonable stable rejection rates over time for chloride for a range of concentrations between 0.01 and 2.5 M. One membrane ran in excess of three months with no apparent loss of usability. This suggests that clay membranes may have a long useable life.

Twenty different hyperfiltration-induced solute precipitation experiments were either attempted or completed and are reported here. The results of these experiments suggest that hyperfiltration-induced solute precipitation is possible, even for very soluble substances such as NaCl. However, the precipitation rates obtained in the laboratory do not appear to be adequate for commercial application at this time. Future experiments will focus on making the clay membranes more compact and thinner in order to obtain higher flux rates. Two alternative methods of removing solutes from solution, for which the New Mexico Tech Research Foundation is preparing patent applications, are also being investigated. These methods will be described in the next annual report after the patent applications are filed.

Technology transfer efforts included two meetings (one in Farmington NM, and one in Hobbs, NM) where the results of this research were presented to independent oil producers and other interested parties. In addition, members of the research team gave seven presentations concerning this research and because of this research project T. M. (Mike) Whitworth was asked to sit on the advisory board for development of a new water treatment facility for the City of El Paso, Texas. Several papers are in preparation for submission to peer-reviewed journals based on the data presented in this report.

TABLE OF CONTENTS

	Page
LIST OF TABLES	vi
LIST OF FIGURES	vii
ACKNOWLEDGEMENTS	ix
EXECUTIVE SUMMARY	1
INTRODUCTION	3
Project Objectives	3
Potential Benefits	3
INTRODUCTION TO CLAY MEMBRANES	6
CLAY MEMBRANE REVERSE OSMOSIS EXPERIMENTS	8
Objectives	8
Previous work	8
Methods	10
Clay preparation	10
Experimental procedure	10
Results	13
Discussion	26
Chloride rejection as a function of pumping rate parallel to the membrane	26
Chloride rejection rate as a function of solution concentration	27
Increase in pump input pressure with increasing solution concentration	28
Membrane stability	29
Membrane efficiency	35
Membrane flow rate	36
Summary and Conclusions	37
SOLUTE PRECIPITATION EXPERIMENTS	38
Objectives	38
Previous Work	38
Theoretical Experiments	38
Methods	43
Clay preparation	43
Experimental cell and flow configuration	44
Procedure for preparing the membrane	46
Procedure for assembling the experimental cell	46
Procedure for setting up the experiment	47
Procedure for running the experiment	47
Procedure for sample dilution	47
Procedure for disassembling the cell	48
Exceptions to the standard procedures	48
Results	50
Discussion	62
Summary and Conclusions	65
TECHNOLOGY TRANSFER	66
Presentations	67
Peer-Reviewed Publications	67

SUMMARY AND CONCLUSIONS.....	68
REFERENCES CITED	69
APPENDIX A: CHEMICAL ANALYSIS FOR WATERDOG PROJECT	72

LIST OF TABLES

	Page
Table 1. Estimated Cost of Wellhead Application of Modified Reverse Osmosis System	4
Table 2. Summary table of cross flow experiments	14
Table 3. Results for Experiment CF-1	15
Table 4. Results for Experiment CF-2	16
Table 5. Clay Bentonite Dissolution Testing Results	16
Table 6. Results for Experiment CF-3	17
Table 7. Results for Experiment CF-4	18
Table 8. Results for Experiment CF-5	19
Table 9. Results for Experiment CF-6	20
Table 10. Results for Experiment CF-7	21
Table 11. Results for Experiment CF-8	22
Table 12. Results for Experiment CF-9	23
Table 13. Results for Experiment CF-10	24
Table 14. Results for Experiment CF-11	25
Table 15. Results for experiment CF-12	26
Table 16. The Salt Rejection Rate (%) vs. Flow Rate (ml/min)	27
Table 17. Summary of Solute Precipitation Experiments	51
Table 18. Results for Experiment H-1	52
Table 19. Results for Experiment H-2	54
Table 20. Results for Experiment H-3	56
Table 21. Results for Experiment H-4	58
Table 22. Data from Experiment H-19	60
Table 23. Data from experiment H-20	60
Table 24. Experimental Results and Calculated Membrane Coefficients.....	64

LIST OF FIGURES

	Page
Figure 1. Conceptual development of a concentration polarization layer.....	7
Figure 2. Typical reverse osmosis pretreatment train.....	9
Figure 3. Freeze-dried bentonite.....	10
Figure 4. Cross-section of experimental cell used in reverse osmosis experiments.....	11
Figure 5. Photograph of cross-flow cell	11
Figure 6. Schematic of experimental setup	12
Figure 7. Photograph of experimental setup.....	13
Figure 8. Error analysis for chloride rejection rate versus total pumping rate	27
Figure 9. Chloride rejection rate as a function of chloride concentration	28
Figure 10. Experimental cell input pressure as a function of chloride concentration	29
Figure 11. Relationship between NaCl concentration and theoretical osmotic pressure	29
Figure 12. Produced water chloride concentration versus time for Experiment 1	30
Figure 13. Produced water chloride concentration versus time for Experiment 2	30
Figure 14. Produced water chloride concentration versus time for Experiment 3	31
Figure 15. Produced water chloride concentration versus time for Experiment 4	31
Figure 16. Produced water chloride concentration versus time for Experiment 5	32
Figure 17. Produced water chloride concentration versus time for Experiment 6	32
Figure 18. Produced water chloride concentration versus time for Experiment 7	33
Figure 19. Produced water chloride concentration versus time for Experiment 8	33
Figure 20. Produced water chloride concentration versus time for Experiment 9	34
Figure 21. Produced water chloride concentration versus time for Experiment 10	34
Figure 22. Produced water chloride concentration versus time for Experiment 11	35
Figure 23. Produced water chloride concentration versus time for Experiment 12	35
Figure 24. Plot of calculated values of the reflection coefficient σ for experiments CF-1 through CF-12.....	36
Figure 25. Graph of theoretical results for scenario where $\sigma = 0.075$ for a 6.0 molar NaCl solution hyperfiltrated through a montmorillonite membrane.....	41
Figure 26. Graph of theoretical results for the second scenario where $\sigma = 0.2$ for a 5.8 molar NaCl solution hyperfiltrated through a montmorillonite membrane.....	42
Figure 27. Graph derived from Equation 9 showing relationship between the reflection coefficient and porosity for montmorillonite (smectite) membranes for differing molar concentrations of NaCl	43
Figure 28. Experimental cell for precipitation experiments	44
Figure 29. Experimental setup for hyperfiltration experiments	45
Figure 30. Photograph of precipitation experiment.....	45
Figure 31. Electron micrograph of NaCl crystals present on the surface of the membrane of Experiment H-1.....	52
Figure 32. Enlargement of a single crystal cluster from Experiment H-1 shown in Figure 31.....	53
Figure 33. Energy dispersive X-ray scan of crystals shown in Figures 31 and 32.....	53
Figure 34. Microprobe scan showing distribution of NaCl crystals across surface of kaolinite membrane from Experiment H-2	55
Figure 35. Energy dispersive X-ray scan of crystals shown in Figure 34.....	55

Figure 36. Microprobe scan showing distribution of NaCl crystals across surface of kaolinite membrane from Experiment H-3	57
Figure 37. Close-up of one of the crystal clusters shown in Figure 36	57
Figure 38. Energy dispersive X-ray scan of crystals shown in Figures 36 and 37	58
Figure 39. Electron micrograph of unknown crystals on surface of membrane from Experiment H-4	59
Figure 40. Photograph taken near the center of the frit in Experiment H-19	61
Figure 41. Group of crystals on the frit of Experiment H-19	61
Figure 42. Crystal on the frit of the control (Experiment H-20)	62

ACKNOWLEDGEMENTS

Many people have helped in this project who are not listed on the cover page. The contributions include assistance with design, procurement, machining, chemical analysis, computer support, technology transfer, bookkeeping, and many other things. They include in no particular order Allan Reisinger, Lynn Brandvold, Terry Thomas, Norton Euart, Floyd Hewitt and other machine shop employees, Jim McLemore, Liz Bustamante, Alex Thyssen, Annette Carroll, Martha Cather, Dave Love, Baolin Deng, Brian McPherson, Nelia Dunbar, Lynn Heizler, Virgil Lueth, Chris McKee, Brenda Parson, Nouraddine Benalil, and student workers supporting us in the laboratories and in computer services. Without all the generous help from everyone, this project would not be possible. Our thanks also goes to the Administration at the New Mexico Institute of Mining and Technology and to our supporters in New Mexico's oil and natural gas industry.

EXECUTIVE SUMMARY

Disposal of produced water can be expensive. In many parts of the country, deep injection wells, or use of produced water for waterflood operations, may not be available disposal options. Therefore, the overall objective of this project is to develop an economical process for treatment of produced water. This research project has two specific objectives. The first is to test clay membranes for reverse osmosis treatment of produced waters. Clay membranes are not expected to need chemical pretreatment and thus should be less expensive to operate than conventional reverse osmosis membranes. The second objective is to test the ability of a system patented by the New Mexico Tech Research Foundation (Patent #6,241,892) to remove salts from reverse osmosis waste streams as a solid. Reduction of the reverse osmosis waste stream to a solid or near-solid will greatly reduce waste disposal costs associated with reverse osmosis treatment of produced waters.

The successful development of the modified reverse osmosis system described in this project will be a significant breakthrough in the field of water treatment. Potential uses extend far beyond treatment of produced waters and have the potential for decreasing operating costs at desalination plants worldwide. The expected compatibility of the proposed technology with the environment, including protection of human health and sensitive ecosystems, is excellent for two reasons: 1) potable water can be produced by this process and 2) for most produced waters, the solid salt waste can either be landfilled or processed for added value.

According to the U. S. Department of Energy, there are about 350 billion barrels of oil reserves remaining in the U. S. On average, about 10 barrels of water are produced for every barrel of oil, which suggests that about 3.5 trillion barrels of water will be produced in order to produce the 350 million bbls of oil. If an average savings of 90% of the disposal cost of produced water is achieved, for coal-bed methane alone, the projected savings on the 340 million bbls of water produced each year is over \$535 million. If the proposed modified reverse osmosis system can be applied successfully to only 5% of these produced waters in the U.S., then the potential long term savings to the U.S. is about \$500 billion.

This report describes work performed during the first year of the project "Modified Reverse Osmosis System for Treatment of Produced Waters." We performed 12 experiments using clay membranes in cross-flow experimental cells. We found that, due to dispersion in the porous frit used adjacent to the membrane, the concentration polarization layer seems to be completely destroyed at low flow rates. This observation suggests that clay membranes used with porous frit material may reach optimum rejection rates at lower pumping rates than those required for use with synthetic membranes. Solute rejection efficiency decreases with increasing solution concentration. For the membranes and experiments reported here, the rejection efficiency ranged from 71% with 0.01 M NaCl solution down to 12 % with 2.3 M NaCl solution. More compacted clay membranes will have higher solute rejection capability. Future experiments will use more compacted clays. The clay membranes used in our experiments were relatively thick (approximately 0.5 mm). The active layer of most synthetic membranes is only 0.04 μm (0.00004 mm), approximately 1250 times thinner than the clay membranes used in these experiments. Yet clay membranes as thin as 12 μm have been constructed (Fritz and Eady, 1985). Since Darcy's law states that the flow through a material of constant permeability is inversely proportional to the material's thickness, then, based on these experimental observations, a very thin clay membrane would be expected to have much higher flow rates than the ones used in these experiments. Future experiments will focus on testing very thin clay membranes. The membranes generally ex-

hibited reasonable stable rejection rates over time for chloride for a range of concentrations between 0.01 and 2.5 M. One membrane ran in excess of three months with no apparent loss of usability. This suggests that clay membranes may have a long useable life.

Twenty different hyperfiltration-induced solute precipitation experiments were either attempted or completed and are reported here. The results of these experiments suggest that hyperfiltration-induced solute precipitation is possible, even for very soluble substances such as NaCl. However, the hyperfiltration-induced precipitation rates for NaCl obtained in our laboratory do not appear to be adequate for commercial application at this time. Future experiments will focus on making the clay membranes more compact and thinner in order to obtain higher flux rates and will investigate ways of improving solute precipitation rates. Two alternative methods of removing solutes from solution, for which the New Mexico Tech Research Foundation is preparing patent applications, are also being investigated. These methods will be described in the next annual report after the patent applications are filed.

Technology transfer efforts included two meetings (one in Farmington NM, and one in Hobbs, NM) where the results of this research were presented to independent oil producers and other interested parties. In addition, members of the research team gave eight presentations concerning this research and, because of the research on this project, T. M. (Mike) Whitworth was asked to sit on the advisory board for development of a new water treatment facility for the City of El Paso, Texas. Several papers are in preparation for submission to peer-reviewed journals based on data presented in this report.

INTRODUCTION

In the United States, more than 20 billion barrels of water are produced each year during oilfield operations. Disposal of produced water can be expensive. For example, produced water in the San Juan Basin of New Mexico and Colorado is currently disposed of by deep-well injection at a cost of approximately \$1.75 per bbl. In other areas the cost of water disposal is typically between \$0.25 and \$0.50 per barrel for pipeline transport and \$1.50 per barrel for trucked water.

In many parts of the country, deep injection wells or use of produced water for water-flood operations may not be available disposal options. The EPA commonly will not allow surface disposal of produced waters because of the high content of dissolved solids. Therefore, in many areas, produced water will need to be treated prior to disposal so that it can meet EPA standards for various uses such as surface disposal, fresh water aquifer recharge, drinking water, irrigation, or release to streams.

Project Objectives

The overall objective of this project is to develop an economical process for treatment of produced water. This research project has two specific objectives. The first is to test clay membranes for reverse osmosis treatment of produced waters. Clay membranes are not expected to need chemical pretreatment and thus should be less expensive than conventional reverse osmosis membranes to operate. The second objective is to test the ability of a system patented by the New Mexico Tech Research Foundation to remove salts from reverse osmosis waste streams as a solid. Reduction of the reverse osmosis waste stream to a solid or near-solid will greatly reduce waste disposal costs associated with reverse osmosis treatment of produced waters.

Potential Benefits

The successful development of the modified reverse osmosis system described in this project will be a significant breakthrough in the field of water treatment. Potential uses extend far beyond treatment of produced waters and have the potential for decreasing operating costs at desalination plants worldwide.

Preliminary estimates developed for produced waters from coal-bed methane wells in the Farmington, New Mexico area (Table 1) suggest that this system has potential water disposal cost savings of between 75% and 95% of current costs. Further cost savings might be obtained if the treated water could be sold for other uses.

The expected compatibility of the proposed technology with the environment, including protection of human health and sensitive ecosystems is excellent for two reasons: 1) potable water can be produced by this process and 2) for most produced waters, the solid salt waste can either be landfilled or processed for added value.

Table 1. Estimated Cost of Wellhead Application of Modified Reverse Osmosis System

Produced Water Volume	5 bpd	50 bpd	100 bpd
Estimated Capital Costs			
Pump	\$300.00	\$700.00	\$1,400.00
Membrane	\$100.00	\$400.00	\$700.00
Precipitator Cell	\$350.00	\$600.00	\$1,200.00
Pre-Filter	\$100.00	\$300.00	\$500.00
Piping, etc.	\$300.00	\$400.00	\$600.00
Installation & Labor	\$300.00	\$500.00	\$900.00
Total Estimated Capital Cost per Installation	\$1,450.00	\$2,900.00	\$5,300.00
Estimated Maintenance and Operating costs for Five-Year Period			
Membrane Replacement	\$150.00	\$450.00	\$900.00
Precipitator Cell Repair and/or Replacement	\$350.00	\$600.00	\$1,200.00
Power (estimated on basis of \$0.10 per KW/hr)	\$1,634.00	\$3,268.00	\$6,536.00
Labor	\$300.00	\$800.00	\$1,100.00
Waste Disposal Costs for Solid Salt (\$10/bbl)	\$32.00	\$320.00	\$640.00
Total Estimated Maintenance and Operating Costs for Five-Year Period	\$3,916.00	\$8,338.00	\$15,676.00
Total Barrels of Produced Water for Five-Year Period	9,125.00	91,250.00	182,500.00
Treatment Cost per Barrel Based on Five-Year Life	\$0.43	\$0.09	\$0.09
Five-Year Cost of Deep Well Injection	\$15,968.75	\$159,687.50	\$319,375.00
Projected Percentage Cost Savings (based on \$1.75/bbl injection costs)	75.48%	94.78%	95.09%

According to the U. S. Department of Energy, there are about 350 billion barrels of oil reserves remaining in the U. S. On average, about 10 barrels of water are produced for every barrel of oil, which suggests that about 3.5 trillion barrels of water will be produced in order to produce the 350 million bbls of oil. If an average savings of 90% of the disposal cost of produced water is achieved, for coal-bed methane alone, the projected savings on the 340 million bbls of water produced each year is over \$535 million. If the proposed modified reverse osmosis system can be applied successfully to only 5% of these produced waters in the U.S., then the potential long term savings to the U.S. is about \$500 billion.

If successful, this modified reverse osmosis system will have application for the desalination of seawater and other waters. According to the American Desalting Association, desalting plants worldwide now have the capacity to produce 3.5 billion gallons a day—nearly enough water to provide 15 gallons per day for every man, woman and child in the United States. About 1,000 desalting plants are currently in operation nationwide. Most U.S. plants are used to clean brackish (moderately salty) groundwater, which is a less expensive process than seawater desalting, or producing highly purified water for industrial use. Although water is relatively inexpensive in the U.S. compared to many other parts of the world, the vagaries of weather, the skyrocketing population growth, and the subsequent increased demand for water in arid or semi-arid areas are contributing to a heightened interest in water desalting as a means to augment existing water supplies. In addition, many communities are turning to desalting as a cost-effective method for complying with increasingly stringent water quality regulations.

Membrane costs represent about 20% of the total operating costs for a desalting plant, and the approximate desalting cost is \$2 per 1000 gallons. Therefore, the total worldwide market

for the proposed membranes would be approximately \$1.4 billion per day or \$511 billion per year. If the proposed project is successful, it is our intention to keep manufacture of the proposed membranes in the U.S.

INTRODUCTION TO CLAY MEMBRANES

Many studies have experimentally confirmed the ability of clays to act as semi-permeable membranes (Marshall, 1948; Wyllie, 1948, 1949; Kemper, 1960, 1961; Berstein, 1960; McKelvey and Milne, 1963; Milne et al, 1963; Milne et al., 1964; Olsen, 1969,1972; Kemper and Rollins, 1966; Kharaka and Berry, 1973; Coplen and Hanshaw, 1973; Srivastava and Jain, 1975; Kharaka and Smalley, 1976; Fritz and Marine, 1983; Benzel and Graf, 1984; Fritz and Eady, 1985; Campbell, 1985; Haydon and Graf, 1986; Demir, 1988; Fritz *et al.*, 1987; Fritz and Whitworth, 1994; Whitworth and Fritz, 1994). Ishiguro, et al. (1995) tested a bentonite membrane formed by smearing some bentonite clay between two pieces of filter paper in a simple cross-flow configuration and achieved NaCl rejections as high as 90.3%. To our knowledge, Ishiguro et al. (1995) is the only clay membrane study that mentions potential commercial use of clay membranes.

Osmotic pressure is generated when a membrane separates solutions of differing concentrations. Water will diffuse through the membrane into the reservoir with the higher solute concentration, thus increasing the pressure in that reservoir. The equilibrium pressure in the reservoir with the higher solute concentration is called the effective osmotic pressure. Some solute will also leave the high solute concentration reservoir, diffuse through the membrane, and enter the lower solute concentration reservoir. Hyperfiltration (also called reverse osmosis) occurs when pressure in excess of osmotic is applied to the membrane and the water flux is forced to reverse direction. Some solute is then rejected by the membrane and accumulates on the higher-pressure side of the membrane. Conventional cross-flow reverse osmosis units prevent this solute buildup by sweeping the high pressure membrane face with a turbulent, high-velocity flux. This is the experimental scenario for the cross-flow reverse osmosis experiments.

When the solute is not swept away and is allowed to build up, hyperfiltration begins with identical solute concentrations on both sides of the membrane at time $t = 0$ (Fig. 1a). Because water passes more easily through the membrane than solute, the solute begins to accumulate at the high-pressure membrane face (Fig. 1b). The zone of increased concentration is called the concentration polarization layer (CPL). As the CPL grows, ever more solute is available at the high-pressure membrane face to enter the membrane. Hence, membrane efficiency decreases and effluent concentration tends to increase concurrently with CPL growth (Fritz and Marine 1983). The concentration at the high-pressure membrane face continues to increase over time as does the width and mass of solute in the CPL (Fig. 1c). Eventually, if no precipitation or chemical reaction occurs, an equilibrium is reached (Fig. 1d) in which the effluent concentration stabilizes at that of the original input concentration. However, concentrations within this CPL can easily reach saturation and/or supersaturation, which results in solute precipitation. When precipitation occurs, the system will reach a steady state in which the effluent concentration is less than the input concentration. It is the equilibrium state in which continuous precipitation occurs that is the objective of the solute precipitation experiments.

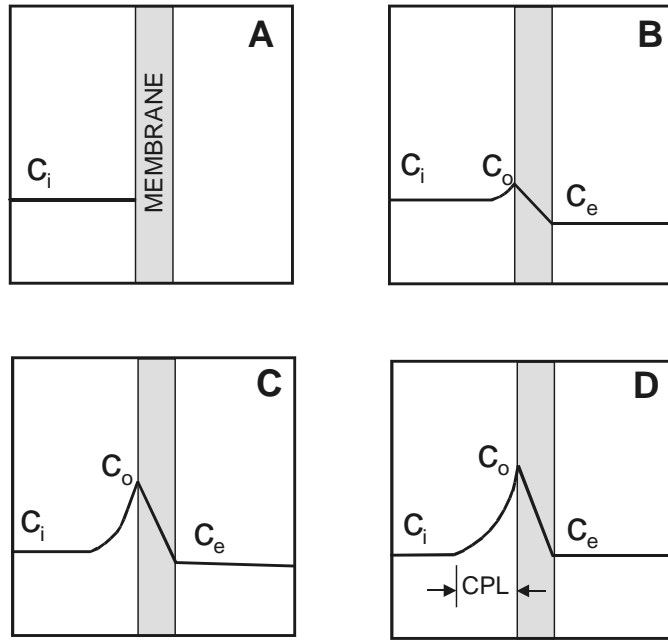


Figure 1. Conceptual development of a concentration polarization layer. The initial conditions (A) are such that the solute is all on the high pressure side of the membrane and the pore fluids within the membrane contain no solute. Some time after solute flux through the membrane begins (B), the concentration at the high pressure membrane face c_o increases because some of the solute is rejected by the membrane. Some solute also begins to pass through the membrane so that the effluent now contains some solute as well. Even later (C), c_o has increased further as has the effluent concentration c_e . At steady-state (D), where no precipitation or chemical reactions are occurring, the input concentration c_i is now equal to c_e and the value of c_o is constant. If saturation is reached or exceeded in the CPL and precipitation occurs, an equilibrium is reached in which $c_e < c_o$, similar to C (Redrawn from Fritz and Marine 1983).

CLAY MEMBRANE REVERSE OSMOSIS EXPERIMENTS

Objectives

The purpose of the experiments described in this section is to test bentonite clay membranes for use in cross-flow reverse osmosis. The goals are to characterize clay membranes using bench-scale experimental cells, test the effect of total pumping rate on clay membrane solute rejection efficiency, and test the effect of the input solution concentration on clay membrane rejection efficiency.

Previous Work

Reverse osmosis as a water treatment technique has been used since the 1950s to produce high quality drinking water that is virtually free from contaminants. During reverse osmosis, salt water under pressure sweeps along one side of a semi-permeable membrane, causing fresh water to diffuse through the membrane, leaving behind a concentrated solution, which must be disposed of as waste. Brackish water reverse osmosis plants typically recover 50 to 80% of the source water while seawater reverse osmosis recovery rates range from 20 to 50%. Costs at large scale reverse osmosis desalination plants typically range from about \$4.00 to \$2.00 per 1000 gallons (\$0.17 to \$0.08 per bbl).

Although successful in a number of desalination plants around the world, application of conventional reverse osmosis to water treatment is still complex. Agents such as precipitates, colloids, microorganisms, and particulates may damage the membranes or effect the reverse osmosis process. Therefore pretreatment is frequently needed (Fig. 2) and pH adjustment is also commonly necessary. Many membranes undergo the least hydrolysis and therefore operate best within the pH range of 4.0 to 5.0, although a range of 5.0 to 6.0 is often used (Montgomery, 1985). Relatively acid pH also helps prevent scaling due to precipitation of slightly soluble calcium carbonate. Figure 2 shows a typical reverse osmosis pretreatment setup. One of the goals of this project is to develop a modified reverse osmosis system that needs no chemical pretreatment.

Cox et al. (1993) examined alternatives to deep-well injection of produced waters including distillation, freeze desalination, reverse osmosis, electrodialysis, ion exchange, and several hybrid systems. They concluded that reverse osmosis and electrodialysis might be applicable for treating produced water from the Fruitland Formation in the San Juan Basin for surface disposal. Their best 1993 projected costs for a combined reverse osmosis/electrodialysis treatment were between \$0.17 and \$0.23 per bbl. In 1993, the projected capital costs for 5000 bpd reverse osmosis/dialysis hybrid systems were as high as \$950,000. High capitalization costs such as these are prohibitive for wellhead installation.

Phillips and Aquatech, in conjunction with the U. S. Department of Energy, installed a reverse osmosis pilot plant in 1992 at Pump Mesa in the San Juan Basin. The 1000 bpd system required pre-filtering, water softening, and pretreatment ahead of the reverse osmosis membrane, and used an evaporator to reduce the concentrate volume. The pilot plant operated for only two months in 1992, but preliminary results suggested that the total treatment costs should be \$1.00 to \$1.20 per bbl in 1993 dollars (Cox et al., 1993; Zimpfer, et al., 1988; and Tait and Brandt, 1992).

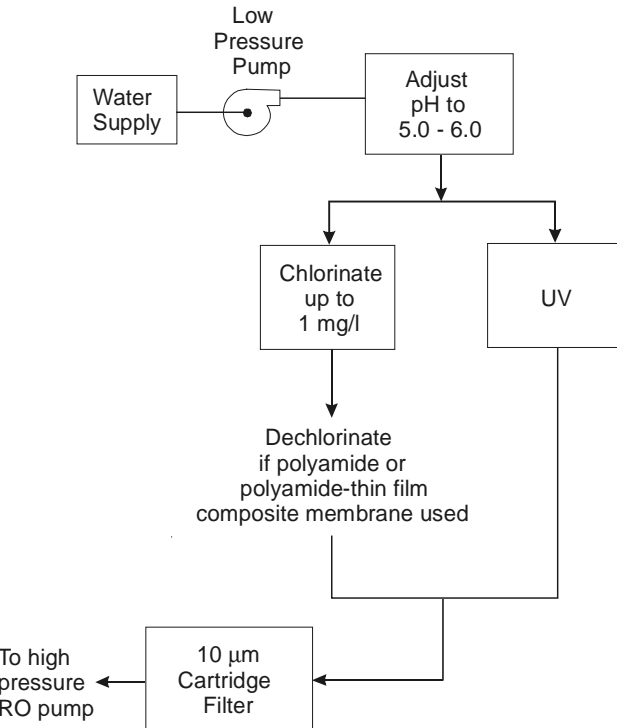


Figure 2. Typical reverse osmosis pretreatment train.

The application of conventional reverse osmosis desalination techniques to treatment of produced waters has the following problems:

- Agents such as precipitates, colloids, microorganisms, and particulates may damage the membranes or affect the reverse osmosis process. Therefore, pretreatment is frequently needed. Pretreatment adds significantly to the operating costs of reverse osmosis.
- The salinity of produced waters is highly variable and ranges from fresh waters (TDS < 500 mg/l) to highly saturated brines (TDS > 200,000 mg/l). Conventional water treatment methods are mostly designed for use with relatively fresh waters, and it is seldom that these methods can be economically applied to waters more saturated than seawater (35,000 mg/l TDS). Reverse osmosis desalination of seawater often requires pressures between 800 and 1200 psi. Reverse osmosis using conventional synthetic membranes with more concentrated brines would require even greater pressures.
- Small-volume reverse osmosis installations cost much more to operate per bbl of treated water than very large volume installations. Many wells do not produce sufficient brine volumes to reach the lower costs associated with larger installations.
- Conventional reverse osmosis produces a significant waste stream that, for brines as concentrated as seawater, can be between 50 and 80% of the total volume treated. These waste brines are expensive to evaporate or otherwise dispose of.

Methods

Clay preparation

The first step in preparation of the bentonite clay for use in the bench-scale cross-flow membrane experiments is to separate the 0.2 μm and smaller size fraction. This was done using standard sedimentation techniques. Following size separation, the clay was freeze-dried using a Model 4.5 Labconco benchtop freeze dryer. The method used was that reported by Whitworth and Fritz (1994). The freeze-dried bentonite is shown in Figure 3. Bentonite is quite fluffy after freeze drying: every 4 grams of freeze-dried bentonite has a volume of approximately 400 ml. After freeze-drying, the clay is stored in nested, tightly sealed ziplock bags to prevent moisture from contacting the clay. The purpose of freeze drying is to remove the moisture content of the clay. Vacuum freeze drying removes non-adsorbed water (Zimmie and Almaleh, 1976, Fritz and Marine, 1983).



Figure 3. Freeze-dried bentonite.

Experimental procedure

A flat-leaf experimental cell was designed for reverse osmosis experiments using clays as the membrane (Figures 4 and 5). This cell, constructed from 316 stainless steel by the machine shop at New Mexico Tech, is designed to operate at hydraulic pressures up to 3000 psi. This cell uses a specially-shaped piston to compress the clay. This feature is not present in commercially available reverse osmosis experimental cells, but is necessary to control the compaction of the clay in these experiments. The membrane area in this cell is 136.5 cm^2 .

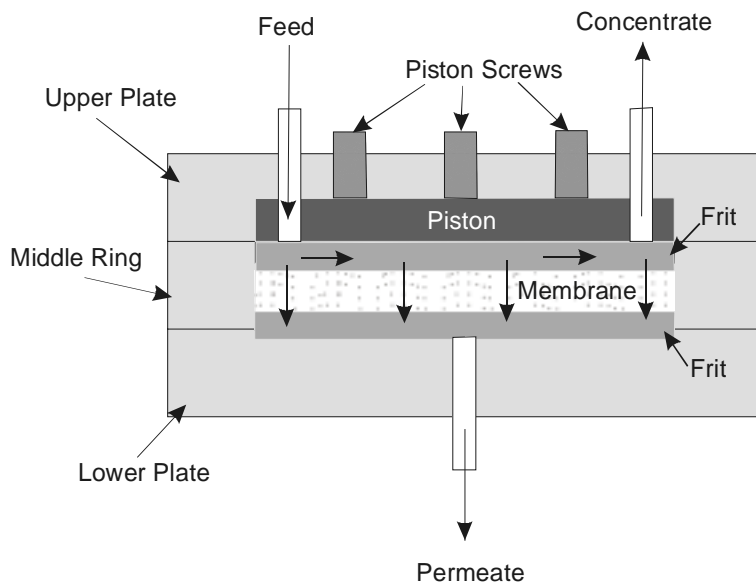


Figure 4. Cross-section of experimental cell used in reverse osmosis experiments. The feed water flows into the feed port into the porous frit overlying the membrane. At this point some of the flow passes through the membrane and some flows parallel to the membrane through the porous frit and exits through the concentrate port. The permeate (the fluid that passes through the membrane) exits at the permeate port.

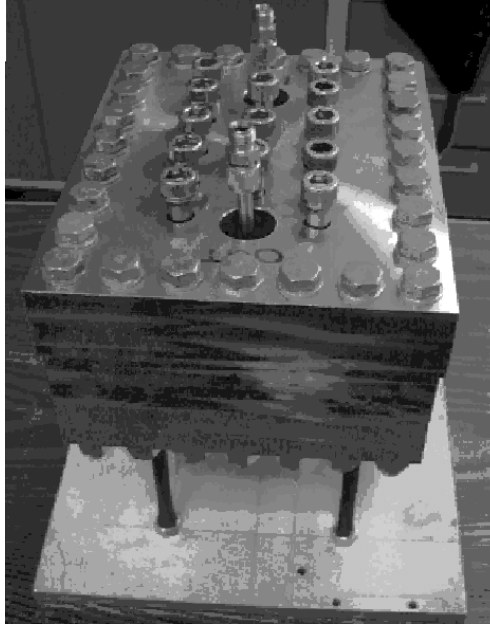


Figure 5. Photograph of cross-flow cell. The three rows of screws near the center bear on the piston. The larger bolts around the edge of the plates hold the assembly together.

The clay membranes were prepared by first pressing a thin layer of freeze-dried clay sandwiched between two Millipore and two Whatman #2 filters in a machined and hardened steel die. The shape of the die exactly matches the recess for the membrane in the experimental cell. The coarser Whatman filter paper is used to protect the Millipore filter paper from damage during pressing. Since the Whatman #2 filter paper damages easily when wet, two additional Millipore filters were used to increase the clay membrane's service lifetime in the laboratory. Exactly 8.00 grams of freeze-dried bentonite were used to prepare each of the membranes used in these experiments. The membranes were each approximately 0.5 mm thick. The dry clay membrane was first compressed at 50,000 pounds total force in a press for about two days, then transferred to the cell and compressed while in the partially assembled cell at 20,000 pounds total force for approximately one hour. Next the cell was quickly assembled and a torque wrench applied to the screws that lock the piston in place until the reading on the torque wrench was 65 pounds per ft. The cell was then set up as shown in Figures 6 and 7 for the experiment.

The pump used in these experiments was a Beckman model 110A. It has a variable flow range from 0 to 594 ml/hr and operates at pressures up to 6000 psi. Before beginning the experimental run, the dry clay membrane was hydrated by passing Type I deionized water into the cell at rate of 0.5 ml/min for two days. During those two days, the inlet and outlet gauge reading were constantly zero and no effluent emerged from the effluent channel in the bottom section of the cell.

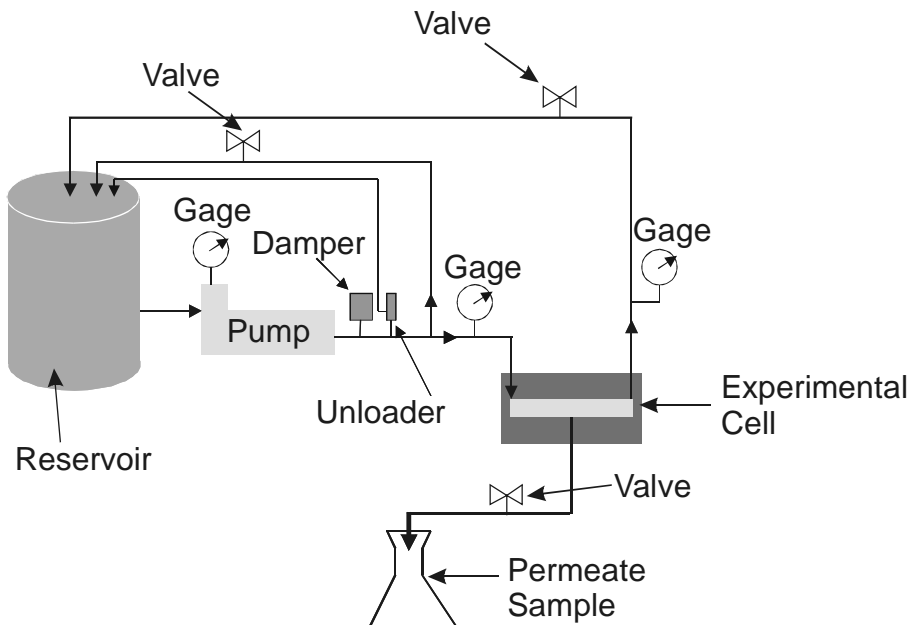


Figure 6. Schematic of experimental setup.



Figure 7. Photograph of experimental setup.

After two days of membrane hydration, the outlet needle valve was slowly adjusted until the inlet pressure was about 600 psi. The samples from the reservoir, outlet, and effluent were taken at almost constant intervals during the experiments.

All the samples were analyzed by ion-chromatography and flow injection analysis (FIA) (See Appendix A). A series of experiments with different NaCl concentrations and different pump flow rates were carried out to investigate the effect of differing solute concentration and flow rate on salt rejection efficiency.

Results

We performed 12 experimental runs with NaCl solutions using commercially available bentonite clay in the cross-flow reverse osmosis cell. These experiments are summarized in Table 2. Two different membranes were used in these experiments. The first membrane was used only for Experiment 1, and the second membrane was used for Experiments 2 through 12.

Table 2. Summary Table of Cross-Flow Experiments

Experiment No.	Pump flow rate (ml/min)	NaCl (M)	Inlet Pressure (psi)	Outlet Pressure (psi)
CF-1	5.7	0.01	550	500
CF-2	0.7	0.1	550	500
CF-3	1.4	0.1	600	400
CF-4	2.1	0.1	600	300
CF-5	0.3	0.1	600	450
CF-6	0.1	0.1	600	500
CF-7	0.7	0.3	600	300
CF-8	0.7	0.6	600	300
CF-9	1.4	1	800	450
CF-10	1.4	1.5	800	450
CF-11	1.4	2	800	450
CF-12	1.4	2.5	800	450

The bentonite clay used to make the first membrane (Experiment CF-1) was obtained from Desert Drilling Fluid Inc., Albuquerque, NM. Upon initial examination of the first effluent data, we thought that there was no rejection of Na^+ because the Na^+ concentration for the reservoir was 215 ppm while the outlet Na^+ concentration was also 215 ppm. X-ray analysis of the clay showed that there was a significant amount of gypsum present in the clay as an impurity. Note that Table 3 shows a high concentration of SO_4^{2-} present in the effluent, but not in the reservoir. From this we deduce that dissolution of gypsum occurs when the NaCl solution passes through the clay membrane. The Ca^{2+} ions freed by dissolution of the gypsum (CaSO_4) are exchanged for the Na^+ ions present on the exchange sites of the clay (a preferred exchange; Whitworth, 1999), and the SO_4^{2-} ions exit the clay into the effluent.

Ion exchange is the substitution of one ion for another on the surface or in the interstices of a crystal. It does not affect crystal structure. Ion exchange in clay minerals occurs because clay minerals can sorb cations and, to a lesser extent, anions from solution. However, when exposed to a different solution, some of these sorbed ions are “exchanged” for other ions. The exchange of ions between the solution and the clay minerals does not affect the crystal structure because the exchangeable ions are held around the outside of the clay mineral structural unit. Clay mineral ion exchange reactions are stoichiometric. In order for a clay to accept x milliequivalents of one ion, it must release x milliequivalents of other ions (i.e. the total charge of the accepted ions must balance the total charge of the released ions). Since ion exchange reactions are stoichiometric, an analysis of the effluent chemistry would incorrectly suggest the presence of Na_2SO_4 as the impurity present in the clay due to the presence of additional released Na^+ ions, instead of the gypsum detected by X-ray analysis. Due to mass balance considerations (Fritz and Whitworth, 1994) it is likely that the actual rejection rates of Na^+ and Cl^- are similar, but this fact is masked by the presence of additional Na^+ ions produced by ion exchange.

This experiment ran for one week. The analyses (Table 3) show a continued decrease in the effluent sulfate concentrations indicating that, while the amount of the gypsum impurity in the clay was decreasing, it was still highly significant at the end of this experimental run.

At the conclusion of this experimental run, we performed dissolution testing on several commercially available bentonites and determined that Wyoming bentonite had the fewest impurities that would produce solutes by dissolution. For the rest of the experiments (CF2–CV12) we changed to a Wyoming sodium bentonite, which did not contain as much gypsum as an impurity.

Table 3 shows the results of the first experiment. This experiment was conducted with 0.01M NaCl solution (416 ppm Cl⁻). The inlet pump pressure was 550 psi and the outlet pump pressure was 500 psi, yielding a 50 psi pressure drop for the flow parallel to the membrane. The rejection rate for chloride at the end of this experiment was about 71%.

Table 3. Results for Experiment CF-1

Time (min)	Permeate			Reservoir		Concentrate		Flow rate through membrane (ml/hr)	Flow rate across membrane (ml/hr)	Inlet Pressure (psi)	Outlet Pressure (psi)
	Na ⁺ (ppm)	Cl ⁻ (ppm)	SO ₄ ²⁻ (ppm)	Na ⁺ (ppm)	Cl ⁻ (ppm)	Na ⁺ (ppm)	Cl ⁻ (ppm)				
0	1123.9	272.5	2624.4	207.5	416.3	215	432.9	0	0	550	500
360	673.8	234.8	1444	207.5	416.3	215	432.9	0.76	20.99	550	500
1110	422.5	212.4	822.9	207.5	416.3	215	432.9	0.69	19.83	550	500
1375	355.8	197.6	637.1	207.5	416.3	215	432.9	0.55	16.39	550	500
1615	227.5	150.3	432.9	207.5	416.3	215	432.6	0.57	15.86	550	500
1855	253.75	153	464.8	207.5	416.3	215	432.6	0.61	15.97	550	500
2455	227.5	153.1	417.5	202.5	407.2	222.5	441.9	0.6	12.05	550	500
2875	218.75	149.8	392	202.5	407.2	222.5	441.9	0.57	11.5	550	500
3875	210	126.6	410	202.5	407.2	222.5	441.9	0.51	10.44	550	500
4295	227.5	111	461	202.5	407.2	222.5	441.9	0.45	9.33	550	500
4535	227.5	109.4	466.8	202.5	407.2	222.5	441.9	0.54	9.33	550	500
4845	210	110.6	438	202.5	407.2	222.5	441.9	0.47	9.15	550	500
5565	201.25	118	402	202.5	407.2	222.5	441.9	0.39	9.15	550	500

Table 4 shows results from Experiment CF-2. This experiment used an 0.95 M NaCl solution (3375 ppm Cl⁻). A new membrane was constructed for this experiment using bentonite (Hydrogel (R), NSF(R) Wyoming Bentonite) from Wyo-Ben Inc., of Billings, Montana⁴. Leach testing was performed on both clays used to make the first and second membranes (Table 5). The tests were conducted for 24 hours, after which the leaching solution was analyzed by ion-chromatography and the Varian[®] SpectrAA-220. Note that the clay containing the gypsum impurity provided 10 mg/l sulfate and 4.8 mg/l sodium to the solution. From a practical standpoint, these added concentrations might not be significant when treating produced waters. However, one of the goals of these experiments is to compare our data with that of Ishiguro et al (1995) who tested the salt rejection capabilities of bentonite clay for low concentration sodium chloride solutions (0.1 M). The solutes leaching from the gypsum-contaminated clay might impede our

ability to make that comparison. The rejection rate for chloride at the end of the experiment was about 68%.

Table 4. Results for Experiment CF-2

Time (min)	Permeate		Reservoir		Concentrate		Flow rate through membrane (ml/hr)	Flow rate across membrane (ml/hr)	Inlet Pressure	Outlet Pressure
	Na ⁺ (ppm)	Cl ⁻ (ppm)	Na ⁺ (ppm)	Cl ⁻ (ppm)	Na ⁺ (ppm)	Cl ⁻ (ppm)			psi	psi
0	0	0	0	0	0	0	0	0	550	500
850	650	797.5	2125	3375	1975	3400	0.27	30	550	500
1570	650	890	2125	3375	1975	3400	0.19	15.6	550	500
2290	800	932.5	2125	3375	2000	3400	0.28	18	550	500
3010	825	970	2125	3375	2000	3400	0.26	35.4	550	500
3730	800	995	2025	3425	1975	3400	0.2	22.8	550	500
4450	775	1015	2025	3425	1975	3500	0.2	7.2	550	500
5170	800	1037.5	2025	3425	1975	3500	0.16	4.2	550	500
5890	800	1070	2025	3425	1975	3350	0.19	4.2	550	500
6610	850	1102.5	2187.5	3350	2025	3500	0.21	4.2	550	500
7330	790	1100	2187.5	3350	2025	3500	0.21	4.2	550	500
8050	792.5	1100	2187.5	3350	2025	3500	0.13	4.2	550	500
8770	805	1125	2187.5	3350	2025	3500	0.2	3.6	550	500
9490	820	1125	2197.5	3350	2405	3350	0.2	3.6	550	500
10210	792.5	1100	2197.5	3350	2405	3350	0.16	3.6	550	500
10930	817.5	1125	2197.5	3350	2405	3350	0.21	3.6	550	500
11650	777.51	1100	2197.5	3350	2405	3350	0.22	3.6	550	500
12370	775	1075	2172.5	3350	2232.5	3375	0.15	60.6	550	500
13090	805.01	1125	2172.5	3350	2232.5	3375	0.18	43.2	550	500
13810	672.5	925	2172.5	3350	2232.5	3375	0.28	43.2	550	500
14530	762.51	1050	2172.5	3350	2232.5	3375	0.23	42.6	550	500
15250	740	1050	2370	3350	2237.5	3350	0.24	42	550	500
15970	717.5	975	2370	3350	2237.5	3350	0.2	42	550	500
16735	782.5	1050	2370	3350	2237.5	3350	0.2	42	550	500
17435	785	1075	2370	3350	2237.5	3350	0.19	42.6	550	500
20153	777.5	1075	2370	3350	2237.5	3350	0.19	42.6	550	500

Table 5. Bentonite Clay Dissolution Testing Results

Clay	Cl mg/(gram clay)	NO ₃ mg/(gram clay)	SO ₄ mg/(gram clay)	Na mg/(gram clay)
Bentonite containing gypsum impurity	1.12	0.38	10	4.8
Wyoming bentonite	0.89	0.68	3.9	1.9
Dialysis (40h)	0.054	N/A	N/A	N/A

Table 6 presents the results for Experiment CF-3. This experiment (as well as the rest of the experiments, through CF-12) used the same membrane (constructed from Wyoming bentonite) as Experiment CF-2. At the end of the run, the reservoir solution remained at approximately the same concentration as that used in Experiment CF-2 and the pumping rate was increased. Note that the inlet pressure for Experiment CF-2 was 550 psi and the outlet pressure was 500 psi, giving a pressure drop parallel to the membrane of 50 psi. In Experiment CF-3, with a higher total flow rate, the inlet pressure was 600 psi and the outlet pressure was 400 psi, giving a pressure drop of 200 psi parallel to the membrane. The measured flow rates were not as steady as desired. No explanation for this was found. Notice that the amount of flow that passed through the membrane near the end of Experiment CF-2 was about 5% and that near the end of Experiment CF-3 was only 0.2%. The chloride rejection rate at the end of Experiment CF-3 was about 66%.

Table 6. Results for Experiment CF-3

Time (min)	Permeate		Reservoir		Concentrate		Flow rate through membrane (ml/hr)	Flow rate across membrane (ml/hr)	Inlet Pressure (psi)	Outlet Pressure (psi)
	Na ⁺ (ppm)	Cl ⁻ (ppm)	Na ⁺ (ppm)	Cl ⁻ (ppm)	Na ⁺ (ppm)	Cl ⁻ (ppm)				
0	0	0	0	0	0	0	0	0	600	400
830	797.5	1100	2250	3400	2300	3400	0.19	82.8	600	400
1550	800	1095	2250	3400	2300	3400	0.14	82.8	600	400
2270	775	1110	2250	3400	2300	3400	0.24	82.8	600	400
2990	750	1085	2250	3400	2300	3400	0.14	82.8	600	400
3710	775	1125	2250	3400	2300	3400	0.23	82.8	600	400
4430	750	1075	2250	3400	2300	3400	0.17	82.8	600	400
5150	750	1062.5	2275	3400	2275	3400	0.18	82.8	600	400
5870	725	1082.5	2275	3400	2275	3400	0.19	82.8	600	400
6590	750	1092.5	2275	3400	2275	3400	0.12	82.8	600	400
7310	725	1075	2275	3400	2275	3400	0.13	82.8	600	400
8150	750	1125	2275	3400	2275	3400	0.16	82.8	600	400
8750	750	1150	2300	3400	2200	3400	0.14	82.8	600	400
9550	725	1112.5	2300	3400	2200	3400	0.15	66	600	400
10910	725	1117.5	2300	3400	2200	3400	0.12	66	600	400
11630	725	1140	2300	3400	2200	3400	0.12	66	600	400
12350	722.24	1158.3	2300	3400	2200	3400	0.08	66	600	400

Experiment CF-4 (Table 7) used the same reservoir solution concentration as that used in both Experiments CF-2 and CF-3, but the pumping rate was once more increased. The pressure drop parallel to the membrane increased to 300 psi but the maximum pressure remained at 600 psi. Again, only about 0.2 % of the flow passed through the membrane. The rejection rate for chloride at the end of the experiment was about 66%.

Table 7. Results for Experiment CF-4

Time (min)	Permeate		Reservoir		Concentrate		Flow rate through membrane (ml/hr)	Flow rate across membrane (ml/hr)	Inlet Pressure (psi)	Outlet Pressure (psi)
	Na ⁺ (ppm)	Cl ⁻ (ppm)	Na ⁺ (ppm)	Cl ⁻ (ppm)	Na ⁺ (ppm)	Cl ⁻ (ppm)				
0	0	0	0	0	0	0	0	0	600	300
720	750	1215	2175	3425	2275	3400	0.12	124.2	600	300
1440	725	1175	2175	3425	2275	3400	0.14	124.2	600	300
2160	725	1165	2175	3425	2275	3400	0.13	124.2	600	300
2880	775	1162.5	2150	3350	2275	3400	0.14	124.2	600	300
3600	800	1180	2150	3350	2275	3400	0.11	103.8	600	300
4320	800	1175	2150	3350	2275	3400	0.12	103.8	600	300
5040	800	1205	2275	3400	2225	3425	0.11	103.8	600	300
5760	800	1212.5	2275	3400	2225	3425	0.13	103.8	600	300
6480	800	1217.5	2275	3400	2225	3425	0.12	102.6	600	300
7200	775	1185	2275	3400	2225	3425	0.1	102.6	600	300
7920	775	1195	2250	3400	2225	3425	0.1	102.6	600	300
8580	775	1200	2250	3400	2225	3425	0.12	102.6	600	300
9300	825	1200	2250	3400	2225	3425	0.16	96.6	600	300
10020	800	1155	2250	3400	2225	3425	0.2	96.6	600	300

Experiment CF-5 (Table 8) used approximately the same reservoir solution concentration as that used in Experiments CF-2 through CF-4 with a lower pumping rate. Pressure drop parallel to the membrane decreased to 250 psi but maximum pressure remained at 600 psi. Volume flow through the membrane was about 0.8 % of the total flow with a rejection rate of about 69%.

Table 8. Results for Experiment CF-5

Time (min)	Permeate		Reservoir		Concentrate		Flow rate through membrane (ml/hr)	Flow rate across membrane (ml/hr)	Inlet Pressure (psi)	Outlet Pressure (psi)
	Na ⁺ (ppm)	Cl ⁻ (ppm)	Na ⁺ (ppm)	Cl ⁻ (ppm)	Na ⁺ (ppm)	Cl ⁻ (ppm)				
0	0	0	0	0	0	0	0	0	600	450
720	700	1082.5	2250	3400	2200	3425	0.23	18.6	600	450
1440	667.5	1067.5	2250	3400	2200	3425	0.16	18.6	600	450
2160	700	1060	2250	3400	2200	3425	0.2	18.6	600	450
2880	675	1097.5	2250	3400	2200	3425	0.18	18.6	600	450
3600	650	1067.5	2325	3425	2082.5	3175	0.26	19.8	600	450
4320	620	1045	2325	3425	2082.5	3175	0.17	19.8	600	450
5055	610	1042.5	2325	3425	2082.5	3175	0.19	19.8	600	450
5940	615	1032.5	2325	3425	2082.5	3175	0.15	19.8	600	450
6555	645	1107.5	2325	3425	2082.5	3175	0.17	19.2	600	450
7200	642.5	1117.5	2332.5	3425	2292.5	3425	0.17	19.2	600	450
7920	635	1097.5	2332.5	3425	2292.5	3425	0.16	19.2	600	450
8640	652.5	1120	2332.5	3425	2292.5	3425	0.15	19.2	600	450
9360	715	1052.5	2332.5	3425	2292.5	3425	0.16	19.8	600	450

In Experiment CF-6 (Table 9) the reservoir solution concentration remained approximately the same as that used in both Experiments CF-2 through CF-5, but the pumping rate was decreased once more. The pressure drop parallel to the membrane decreased to 100 psi but the maximum pressure remained at 600 psi. Volume flow through the membrane was about 2% of the total flow and rejection rate for chloride at the end of the experiment was about 68%.

Table 9. Results for Experiment CF-6

Time (min)	Permeate		Reservoir		Concentrate		Flow rate through membrane (ml/hr)	Flow rate across membrane (ml/hr)	Inlet Pressure (psi)	Outlet Pressure (psi)
	Na ⁺ (ppm)	Cl ⁻ (ppm)	Na ⁺ (ppm)	Cl ⁻ (ppm)	Na ⁺ (ppm)	Cl ⁻ (ppm)				
0	0	0	0	0	0	0	0	0	600	500
720	772.5	1157.5	2265	3425	2385	3475	0.22	7.8	600	500
1440	682.5	1062.5	2265	3425	2385	3475	0.21	7.8	600	500
2160	722.5	1080	2265	3425	2385	3475	0.15	7.8	600	500
2880	700	1070	2265	3425	2385	3475	0.14	7.8	600	500
3600	712.5	1085	2197.5	3450	2277.5	3500	0.12	7.8	600	500
4320	702.5	1100	2197.5	3450	2277.5	3500	0.13	7.8	600	500
5040	717.5	1115	2197.5	3450	2277.5	3500	0.13	7.2	600	500
5790	732.5	1142.5	2197.5	3450	2277.5	3500	0.22	7.2	600	500
6480	510	777.5	2197.5	3450	2277.5	3500	0.19	7.2	600	500
7200	677.5	1080	2285	3350	2077.5	3300	0.28	7.2	600	500
7920	667.5	1050	2285	3350	2077.5	3300	0.18	7.2	600	500
8640	530	830	2285	3350	2077.5	3300	0.17	7.2	600	500
9360	710	1092.5	2285	3350	2077.5	3300	0.15	7.2	600	500
10080	710	1085	2285	3350	2077.5	3300	0.12	7.2	600	500

In Experiment CF-7 (Table 10), reservoir solution concentration was increased to approximately 0.3 M (10528 ppm Cl⁻). A 300 psi pressure drop occurred parallel to the membrane in this experiment, while inlet pressure remained at 600 psi. The flow volume that passed through the membrane was about 0.3% and rejection rate for chloride at the end of the run was about 60%.

Table 10. Results for Experiment CF-7

Time (min)	Permeate		Reservoir		Concentrate		Flow rate through membrane (ml/hr)	Flow rate across membrane (ml/hr)	Inlet Pressure (psi)	Outlet Pressure (psi)
	Na ⁺ (ppm)	Cl ⁻ (ppm)	Na ⁺ (ppm)	Cl ⁻ (ppm)	Na ⁺ (ppm)	Cl ⁻ (ppm)				
0	0	0	0	0	0	0	0	0	600	300
510	732.14	928.57	6541.7	10528	6583	10556	0.09	45	600	300
1230	750	972.22	6541.7	10528	6583	10556	0.13	45	600	300
1950	1388.9	2041.7	6541.7	10528	6583	10556	0.09	45	600	300
2670	2236.1	3436.1	6541.7	10528	6640	10500	0.16	45	600	300
3000	2662.5	3938.9	6541.7	10528	6640	10500	0.17	44.4	600	300
3690	2787.5	4183.3	6541.7	10528	6640	10500	0.13	44.4	600	300
4410	2943.8	4527.8	6541.7	10528	6640	10500	0.14	44.4	600	300
5190	3068.8	4627.8	6541.7	10528	7000	10500	0.14	44.4	600	300
5910	3375	4672.2	6541.7	10528	7000	10500	0.11	44.4	600	300
6600	3506.3	4700	6541.7	10528	7000	10500	0.1	44.4	600	300
7290	3287.5	5172.2	6650	10360	6690	10410	0.08	44.4	600	300
7980	3412.5	4666.7	6650	10360	6690	10410	0.07	44.4	600	300
8700	3256.3	4800	6650	10360	6690	10410	0.09	44.4	600	300
9420	3356.3	5022.2	6650	10360	6690	10410	0.1	43.8	600	300
10140	3475	5272.2	6740	10420	6530	10450	0.11	43.8	600	300
10860	3312.5	5077.8	6740	10420	6530	10450	0.19	43.8	600	300
11580	3550	4961.1	6740	10420	6530	10450	0.14	43.8	600	300
12330	2993.8	4127.8	6740	10420	6530	10450	0.13	43.8	600	300

In Experiment CF-8 (Table 11) NaCl concentration was increased to approximately 0.6 M (20880 ppm Cl⁻). The inlet pressure was 600 psi and the outlet pressure was 300 psi. The pressure drop parallel to the membrane was 300 psi. The percentage of total flow passing through the membrane at the end of the experiment was about 0.6 % and the rejection rate for chloride at the end of the experiment was 42%.

Table 11. Results for Experiment CF-8

Time (min)	Permeate		Reservoir		Concentrate		Flow rate through membrane (ml/hr)	Flow rate across membrane (ml/hr)	Inlet Pressure (psi)	Outlet Pressure (psi)
	Na ⁺ (ppm)	Cl ⁻ (ppm)	Na ⁺ (ppm)	Cl ⁻ (ppm)	Na ⁺ (ppm)	Cl ⁻ (ppm)				
0	0	0	0	0	0	0	0	0	600	300
410	3060	5360	13120	20880	13600	20960	0.09	45.6	600	300
1040	3087.5	5562.5	13120	20880	13600	20960	0.12	45.6	600	300
1760	4737.5	8525	13120	20880	13600	20960	0.14	45.6	600	300
2480	6537.5	11225	13120	20880	13600	20960	0.23	45.6	600	300
3200	7000	12063	13620	20820	13940	21020	0.17	44.4	600	300
3920	6850	11900	13620	20820	13940	21020	0.24	44.4	600	300
4640	7050	12200	13620	20820	13940	21020	0.16	44.4	600	300
5360	7525	11550	13620	20820	13940	21020	0.18	44.4	600	300
6080	7612.5	11925	13500	20960	13600	21000	0.15	44.4	600	300
6800	8175	12550	13500	20960	13600	21000	0.21	44.4	600	300
7520	8537.5	13225	13500	20960	13600	21000	0.17	44.4	600	300
8240	7962.5	12838	13500	20960	13600	21000	0.3	44.4	600	300
8960	7675	11938	14540	21200	13200	20880	0.22	44.4	600	300
9680	7700	12363	14540	21200	13200	20880	0.3	44.4	600	300
10400	8150	12325	14540	21200	13200	20880	0.21	44.4	600	300
11120	8200	12300	14540	21200	13200	20880	0.25	44.4	600	300

In Experiment CF-9 (Table 12) , solution concentration was increased to approximately 1.0M NaCl (35,965 ppm Cl⁻). The inlet pressure was increased to 800 psi for this run with outlet pressure at 450 psi. The pressure drop parallel to the membrane was 350 psi. The pumping rate, 1.4 ml/min, was approximately twice that used in Experiment CF-8. Only 0.2 % of the total flow passed through the membrane. The rejection rate for chloride at the end of the experiment was 26%.

Table 12. Results for Experiment CF-9

Time (min)	Permeate	Reservoir	Concentrate	Flow rate through membrane (ml/hr)	Flow rate across membrane (ml/hr)	Inlet Pres- sure psi	Outlet Pres- sure psi
	Cl ⁻ (ppm)	Cl ⁻ (ppm)	Cl ⁻ (ppm)				
0	0	0	0	0	0	800	450
840	14777	36227	35965	0.05	89.4	800	450
2220	16937	36227	35965	0.16	89.4	800	450
2880	21634	36227	35965	0.27	89.4	800	450
3600	23564	36227	35965	0.19	89.4	800	450
4320	24434	36059	35882	0.17	85.2	800	450
5040	24590	36059	35882	0.22	85.2	800	450
5760	26130	36059	35882	0.14	85.2	800	450
6420	25404	36059	35882	0.17	85.2	800	450
7200	25729	36000	35527	0.20	81.6	800	450
7920	25003	36000	35527	0.20	81.6	800	450
8640	25908	36000	35527	0.22	81.6	800	450
9360	25793	36000	35527	0.20	81.6	800	450
10080	25826	35573	36220	0.20	85.2	800	450
11460	25819	35573	36220	0.16	85.2	800	450
12240	25621	35595	35681	0.25	85.2	800	450
12960	25961	35595	35681	0.13	88.2	800	450
14400	25530	35595	35681	0.16	88.2	800	450
15840	26831	35595	35681	0.18	85.2	800	450

In Experiment CF-10 (Table 13) solution concentration was increased to approximately 1.5 M (54,137 ppm Cl⁻). The inlet pump pressure was 800 psi and the outlet pressure was 450 psi. The pressure drop parallel to the membrane was 350 psi. The pumping rate, at 1.4 ml/min, was similar to Experiment CF-9. About 0.2 % of the total flow passed through the membrane. The rejection rate for chloride at the end of the experiment was %.

Table 13. Results for Experiment CF-10

Time (min)	Permeate	Reservoir	Concentrate	Flow rate through membrane (ml/hr)	Flow rate across membrane (ml/hr)	Inlet Pres- sure (psi)	Outlet Pres- sure (psi)
	Cl ⁻ (ppm)	Cl ⁻ (ppm)	Cl ⁻ (ppm)				
0	0	0	0	0	0	800	450
810	26059	53787	54137	0.17	73.2	800	450
1530	30873	53787	54137	0.17	73.2	800	450
2310	33482	53787	54137	0.12	73.2	800	450
2970	36797	53787	54137	0.21	73.2	800	450
3690	41791	54330	54314	0.31	86.4	800	450
4410	41473	54330	54314	0.18	86.4	800	450
5040	41819	54330	54314	0.18	86.4	800	450
5850	39303	54330	54314	0.19	86.4	800	450
6630	43284	54855	55714	0.21	86.4	800	450
7320	42763	54855	55714	0.19	86.4	800	450
8010	42358	54855	55714	0.23	86.4	800	450
8800	41683	54855	55714	0.14	86.4	800	450

In Experiment CF-11 (Table 14) solution concentration was increased to approximately 2M (69661 ppm Cl⁻) for this run. The inlet pressure and outlet pressure were 800 and 450 psi respectively, with pump rate of 1.4 ml/min. About 0.2 % of the total flow passed through the membrane. The rejection rate for chloride near the end of the experimental run was 14%.

Table 14. Results for Experiment CF-11

Time (min)	Permeate	Reservoir	Concentrate	Flow rate through membrane (ml/hr)	Flow rate across membrane (ml/hr)	Inlet Pres- sure psi	Outlet Pres- sure psi
	Cl ⁻ (ppm)	Cl ⁻ (ppm)	Cl ⁻ (ppm)				
0	0	0	0	0	0	800	450
450	46425	70348	69661	0.16	88.8	800	450
1140	46091	70348	69661	0.13	8880	800	450
1800	50596	70348	69661	0.14	88.8	800	450
2520	55521	69869	69727	0.14	88.8	800	450
3240	57339	69869	69727	0.18	89.4	800	450
3960	58678	69869	69727	0.18	89.4	800	450
4680	57660	70285	68701	0.19	89.4	800	450
5370	59540	70285	68701	0.18	89.4	800	450
6120	58766	70285	68701	0.16	88.2	800	450
6840	58578	68729	68701	0.18	88.2	800	450
7560	59551	68729	68701	0.17	88.2	800	450
8280	59116	68729	68701	0.13	88.2	800	450

In Experiment CF-12 (Table 15) solution concentration was increased to approximately 2.5 M (81,510 ppm Cl⁻). The inlet pressure and outlet pressure were 800 and 450 psi respectively. The pump rate was approximately 1.4 ml/min, the same as that used in experiment CF-10, but varied a little more during the run. About 0.2% of the total flow passed through the membrane. The rejection rate for chloride near the end of the experimental run was 12%.

Table 15. Results for Experiment CF-12

Time (min)	Permeate	Reservoir	Concentrate	Flow rate through membrane (ml/hr)	Flow rate across membrane (ml/hr)	Inlet Pres- sure (psi)	Outlet Pres- sure (psi)
	Cl ⁻ (ppm)	Cl ⁻ (ppm)	Cl ⁻ (ppm)				
0	0	0	0	0	0	800	450
720	62134	80995	80215.9	0.19	87.6	800	450
1440	62747	80995	80215.9	0.14	87.6	800	450
1950	68152	80995	80215.9	0.16	81	800	450
2820	70511	81324	80215.9	0.13	81	800	450
3420	71874	81324	80215.9	0.15	81	800	450
4140	69859	81324	80215.9	0.11	81	800	450
4860	70927	81510	80215.9	0.16	90.6	800	450
5580	70988	81510	80215.9	0.17	90.6	800	450
6270	71579	81510	80215.9	0.13	88.8	800	450

Discussion

The 12 experiments with bentonite membranes were designed to 1) test the chloride rejection as a function of flow rate and 2) test the chloride rejection rate as a function of concentration. The experiments on chloride rejection as a function of flow rate included Experiments CF-2 through CF-6, and the experiments on chloride rejection as a function of solute concentration include Experiments CF-2, CF-3 and CF-7 through CF-12.

Chloride rejection as a function of pumping rate parallel to the membrane

The purpose of these experiments was to determine if a concentration polarization layer (CPL) forms adjacent to the membrane during solute rejection and what total pumping rates are necessary to adequately diminish the CPL in order to achieve optimum rejection rates. If formation of a concentration polarization layer has a negative impact on solute rejection. In this series of experiments, the pump rates were varied between 0.1 ml/min and 1.7 ml/min. Table 16 shows the rejection rate as a function of the total pumping rate.

Table 16. Salt Rejection Rate (%) vs. Flow Rate (ml/min)

Experiment	Flow rate ml/min	Cation Na ⁺		Anion Cl ⁻	
		Avg., ppm	Rejection Rate (%)	Avg., ppm	Rejection Rate (%)
CF-6	0.1	705	68.26	1092.5	67.59
CF-5	0.3	638.29	71.27	1076.2	68.08
CF-2	0.7	720.71	67.65	1062.1	68.5
CF-3	1.4	711.68	67.96	1106.6	67.17
CF-4	2.1	751.53	66.17	1188.8	64.74

*The reservoir average concentration for Na⁺ 2221.35 ppm and Cl⁻ 3371.15 ppm respectively

Changing the total pumping rate had little impact on the rejection rate. Examining the precision of the chemical analyses (Appendix A) we see that the average precision of chloride analyses was 0.5%, which, in the concentration range of these results, will affect the rejection rate by approximately $\pm 0.3\%$. Thus, a simple error bar analysis (Figure 8) shows that there was no statistical difference in the rejection rate for the lower flow rates and that the rejection rate was slightly, though significantly lower for the highest total pumping rate. Chloride is the best indicator because it is a conservative solute and does not participate significantly in ion exchange. It is possible that the Na analyses are at least slightly affected by ion exchange within the clay membrane—especially in the earliest effluents. The results suggest that when a porous frit is used with a clay membrane, instead of the plastic waffle-shaped grid used with synthetic membranes, that high flow rates may not be needed to achieve optimum rejection rates. This is thought to occur because the frit material acts like a porous media and the dispersion effects act to destroy the CPL at lower flow rates than might otherwise be expected. At higher flow rates, the flow within the pores of the frit becomes turbulent, and the transfer of fluid to the membrane

interface becomes more difficult. This is reflected in the lower flow rate of fluid through the membrane when the total pumping rate was 2.1 ml/min, as compared to the other experiments.

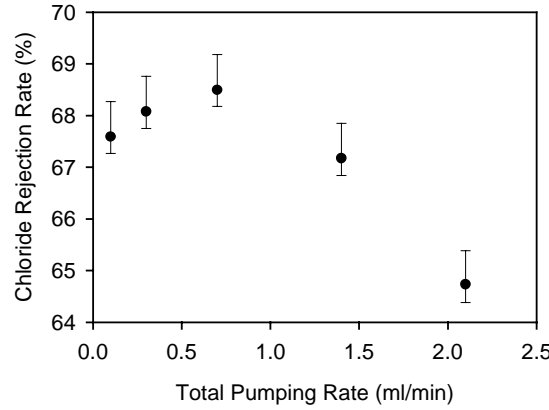


Figure 8. Error analysis for chloride rejection rate versus total pumping rate.

The observation that lower flow rates provide optimum rejection rates may prove beneficial because it suggests that clay membranes used with porous frit material may reach optimum rejection rates at lower pumping rates than must be used with synthetic membranes. The results of these experiments suggest no significant concentration polarization is occurring. If concentration polarization were occurring, the rejection efficiency would decrease with flow rate below a threshold flow rate.

Chloride rejection rate as a function of solution concentration

These experiments (CF-1, CF-3, and CF-7 through CF-12), as much as possible, used the same total pumping rate with solution concentration varying between 0.01M and 2.3 M NaCl. The average rejection rate is plotted as a function of concentration in Figure 9. Notice that the chloride rejection rate drops off as the chloride concentration increases in the feed water. This result is predicted by Fritz (1986). Both of the membranes (that used in Experiment CF-1, and the other of Wyoming bentonite used in the rest of the experiments) were compacted to similar levels. Fritz and Marine (1983) showed that clay membrane efficiency increases as compaction increases. Future experiments will be done at higher compaction levels and should exhibit even higher rejection rates.

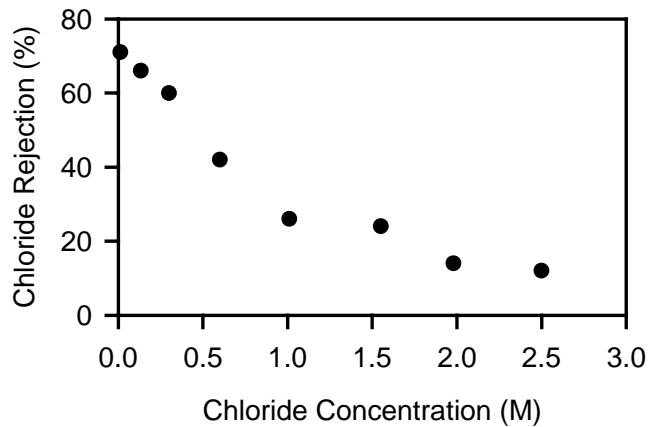


Figure 9. Chloride rejection rate as a function of chloride concentration.

Increase in pump input pressure with increasing solution concentration

Osmotic pressure increases with increasing solution concentration. Therefore, the required pressure to operate any membrane should increase as feed water concentrations increase. That was the case observed with the bentonite membranes tested. Figure 10 shows that as the feed water solution concentration increased, the cell input pressure generally increased as well. Note however, that the data shows only a general trend.

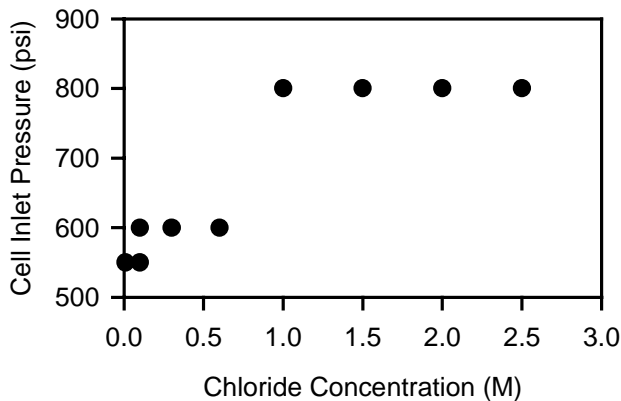


Figure 10. Experimental cell input pressure as a function of chloride concentration.

The relationship between NaCl concentration and the theoretical osmotic pressure (i.e., the osmotic pressure exhibited by a perfect membrane where $\sigma = 1.0$) is shown in Figure 11. Synthetic membranes designed for seawater desalination require feed pressures of 800 to 1000 psi. Seawater has a dissolved solute concentration of about 35000 ppm or 1 mole per liter. The bentonite membranes used in these experiments needed a feed pressure of 800 psi for solution

concentrations between 1 and 2.5 molar. The clay membranes are very thick (approximately 0.5 mm). The active layer of most synthetic membranes is only 0.04 μm (0.00004 mm), approximately 1250 times thinner than the clay membranes used in these experiments. Yet clay membranes as thin as 12 μm have been constructed (Fritz and Eady, 1985). Since Darcy's law states that the flow through a material of constant permeability is inversely proportional to its thickness, then, based on these experimental observations, a very thin clay membrane would be expected to have much higher flow rates than the ones used in these experiments. Future experiments will focus on testing very thin clay membranes.

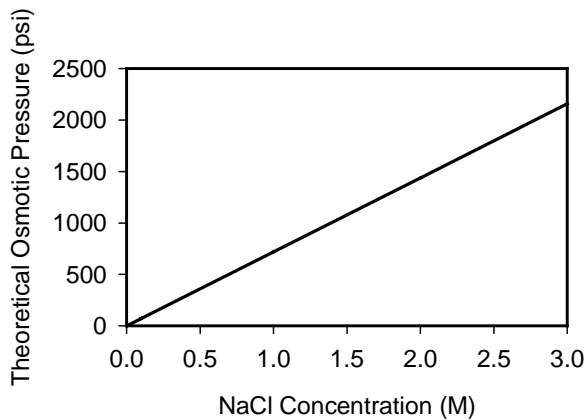


Figure 11. Relationship between NaCl concentration and theoretical osmotic pressure.

Membrane stability

A major concern for application of any membrane to water treatment is the stability of the membrane. The tests presented in this report are relatively short term, yet a single bentonite membrane was used for a number of experiments over a period of over three months with no evidence of failure or significant loss of clay due to hydrolysis.

Another concern is how consistently the membrane performs over a period of time. Each of the 12 experimental runs reported took approximately one week or more. The chloride concentrations of the produced water for each experiment are shown in Figures 12 through 23. The first experiment (Figure 12) shows a decrease in the permeate chloride concentration over a period of about 70 hours until a steady state was reached. This decreasing permeate concentration is attributed to dissolution of minerals from the clay. The feed water NaCl concentration in this experiment was very low—only 0.01 M. As we stated in the “Results” section, the clay used in this experiment was replaced with a purer bentonite for the rest of the experiments.

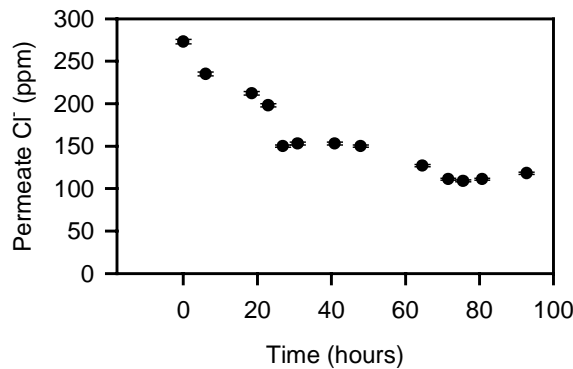


Figure 12. Produced water chloride concentration versus time for Experiment CF-1.

Note that Experiment 2 (Figure 13) exhibits some instability in the late part of the run. This may be attributable to the large variation in total pumping rate that occurred at this time. Increasing the pumping rate seemed to slightly decrease the chloride rejection.

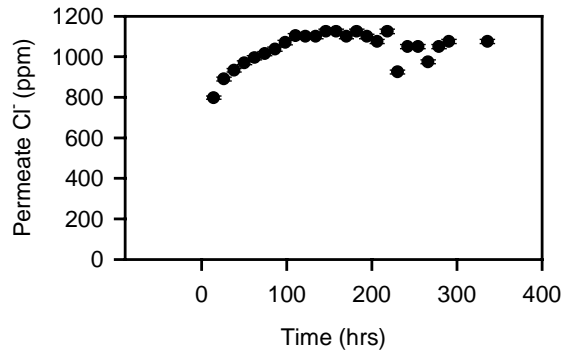


Figure 13. Produced water chloride concentration versus time for Experiment CF-2.

In experiment CF-3 (Figure 14), the chloride rejection shows a stable trend. This is the steady rejection rate sought after in reverse osmosis operations. Experiment CF-4 (Figure 15) shows a very similar trend.

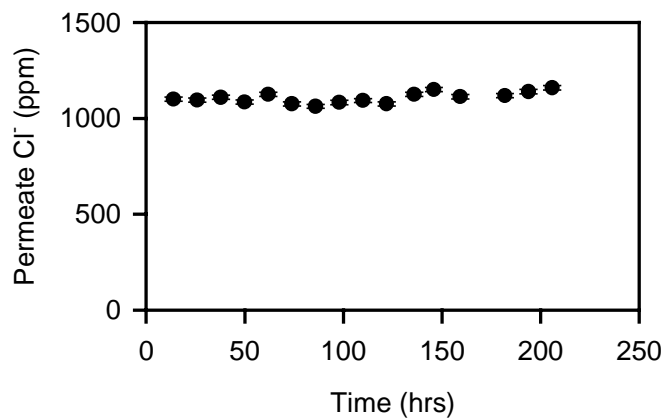


Figure 14. Produced water chloride concentration versus time for Experiment CF-3.

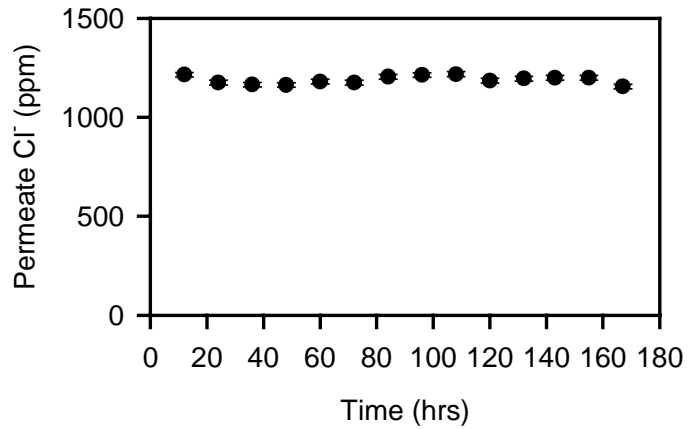


Figure 15. Produced water chloride concentration versus time for Experiment CF-4.

The chloride rejection trend in Experiment CF-5 (Figure 16) is also reasonably stable. However, Experiment CF-6 (Figure 17) shows two outliers in an otherwise stable run. The pumping rate and pressures were steady during this run. Unless these outliers are due to analytical or sample collection or dilution errors, we have no explanation for them.

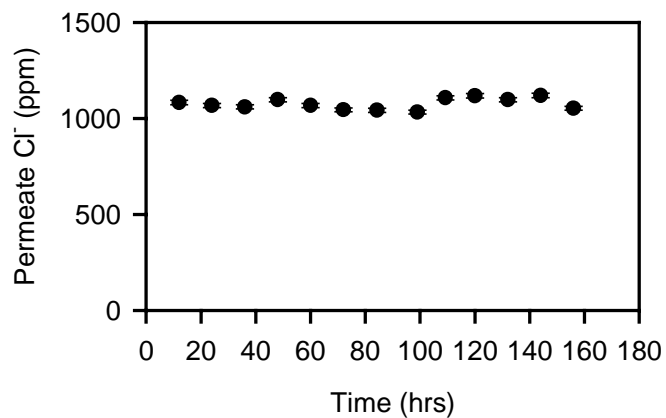


Figure 16. Produced water chloride concentration versus time for Experiment CF-5.

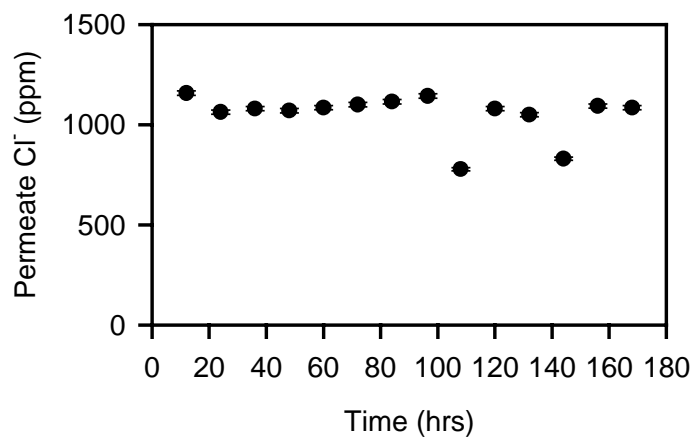


Figure 17. Produced water chloride concentration versus time for Experiment CF-6.

In Experiment CF-7 (Figure 18) the solution concentration was increased from 0.1 M to 0.3 M. The data clearly show the displacement of the old solution from within the membrane and membrane cell with the new. Notice that it takes over 50 hours to effect a reasonably complete replacement. After that, the data is not as steady as the previous runs with 0.1 M NaCl, but does appear to reach a steady state. In Experiment CF-8 (Figure 19) the 0.3 M NaCl solution was displaced with a 0.6 M NaCl solution. This displacement took a little less than 50 hours. There is significant variability in the rejection rate for chloride in this run, but the overall trend is flat.

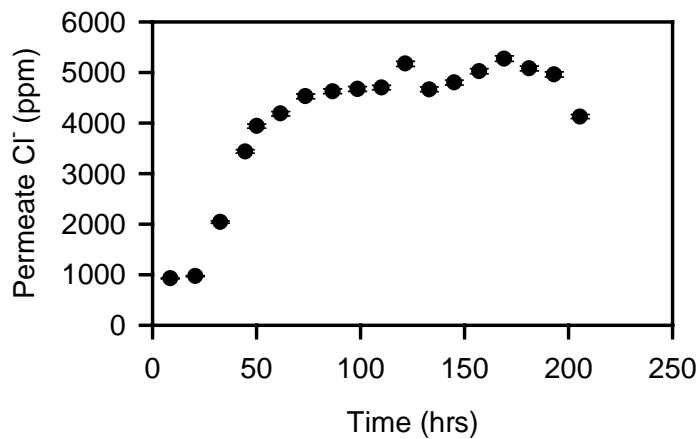


Figure 18. Produced water chloride concentration versus time for Experiment CF-7.

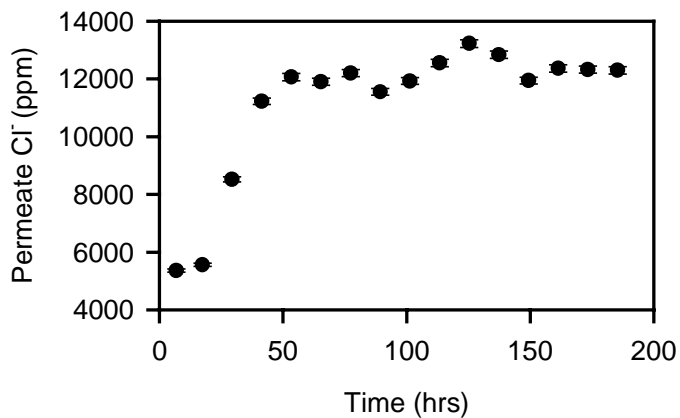


Figure 19. Produced water chloride concentration versus time for Experiment CF-8.

In Experiment CF-9 (Figure 20), the 0.6 M NaCl solution was displaced with a 1.9 M NaCl solution. The displacement took approximately 75 hours. After that time the trend in chloride rejection was reasonably stable. The last data point may be an outlier. Experiment CF-10 (Figure 21) displaced the 1.0 M solution with 1.5 M NaCl solution. This displacement took about 65 hours. With the exception of a single outlier, the rejection rate for chloride after that time is reasonably stable.

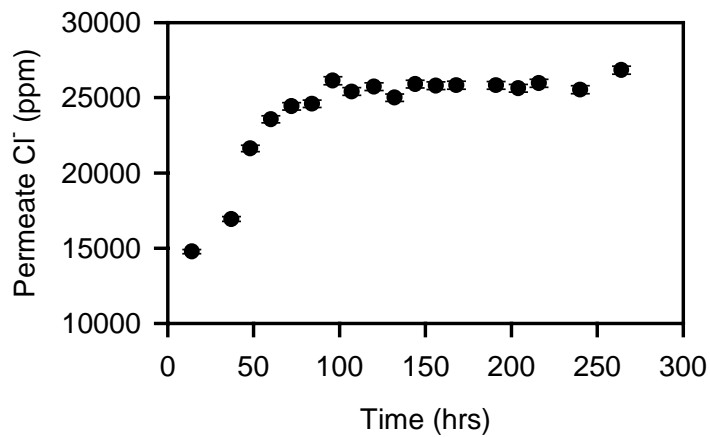


Figure 20. Produced water chloride concentration versus time for Experiment CF-9.

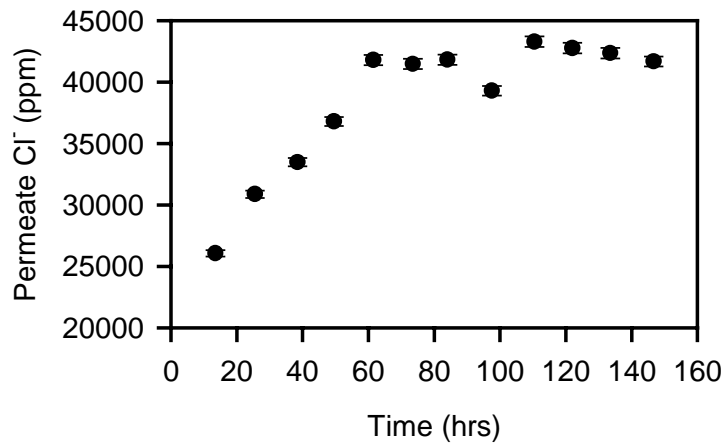


Figure 21. Produced water chloride concentration versus time for Experiment CF-10.

In Experiment CF-11 (Figure 22), the 1.5 M NaCl solution was displaced with a 2.0 M NaCl solution. It took approximately 60 hours to complete the displacement. After 60 hours, the rejection rate was fairly stable. Experiment CF-12 (Figure 23) displaced the 2.0 M NaCl solution with 2.5 M NaCl solution. This displacement appeared to have only taken about 20 hours, after which the permeate chloride concentration was quite stable.

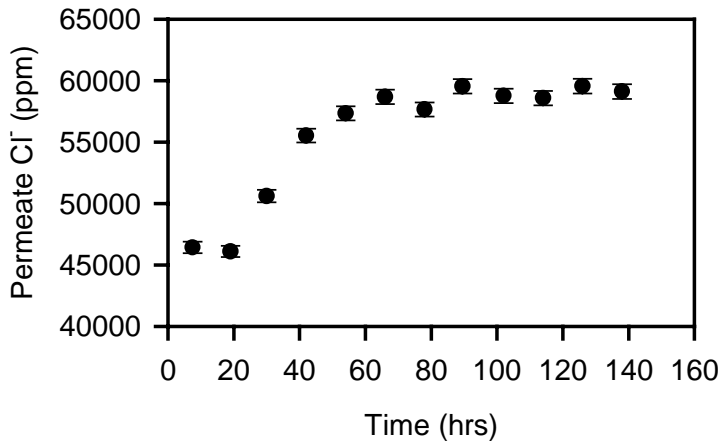


Figure 22. Produced water chloride concentration versus time for Experiment CF-11.

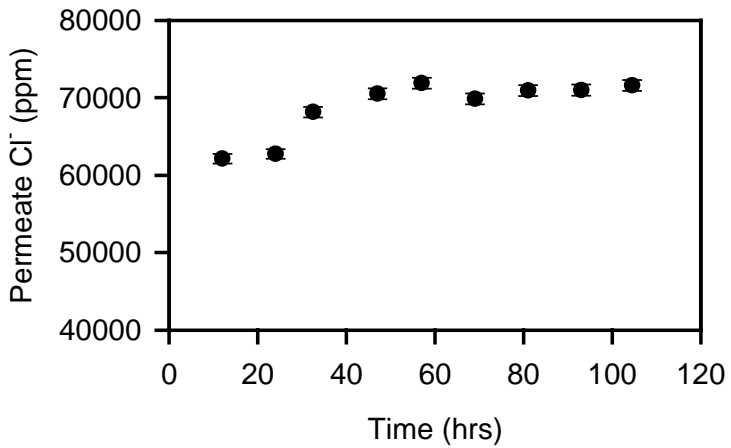


Figure 23. Produced water chloride concentration versus time for Experiment CF-12.

Membrane efficiency

Are the observed clay membrane separation efficiencies representative of the best that might be expected from bentonite membranes? To answer that question we will first calculate the osmotic efficiency σ of the clay membranes for each experiment using the relationship $\sigma = (c_e - c_o) / (c_o + c_e)$ (Fritz and Marine, 1983) where c_o is the reservoir concentration and c_e is the permeate concentration. The results of these calculations are shown in Figure 24. Figure 24 shows that σ generally decreases with increasing concentration. Since the same bentonite membrane was used in experiments CF2 through CF-12, all but the highest point on the graph are data for a single membrane. The frictional coefficient membrane model presented by Fritz and Marine (1983) predicts a porosity in the range of 80%+ for the two clay membranes used in these experiments. The model also predicts that more compacted clays should have significantly greater

separation efficiencies than reported in these experiments. Future experiments will focus on obtaining greater levels of membrane compaction and thus higher separation efficiencies.

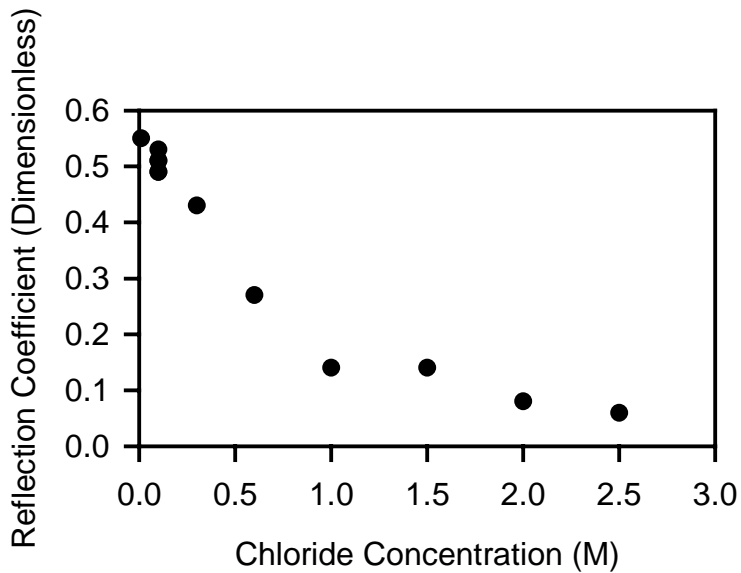


Figure 24. Plot of calculated values of the reflection coefficient σ for experiments CF-1 through CF-12. The reflection coefficient is a unitless number that describes the osmotic efficiency of membranes. A value of 0.5 indicates that the membrane is capable of maintaining 50% of the theoretical maximum osmotic pressure.

Membrane flow rate

The flow rate through any material is directly proportional to its thickness. It was not possible in these experiments to obtain an accurate measurement of the thickness of the clay membranes, but upon removal the membrane thickness was estimated to be a maximum of 0.05 cm. The actual membrane thickness under compression in the cell would have been as much as 10 to 30% less because the clay rebounds or swells when the confining pressure is released. Future experiments will be designed to more accurately measure the membrane thickness.

The flow rates through the approximately 0.5mm thick bentonite membranes, depending on experimental conditions, ranged between 0.2 and 5% of the total flow. Since the relationship between flow rate and pressure is linear, when all other factors, such as solution concentration, remain constant, thinning the membranes should result in significantly increased permeate flux for the same conditions. As an example, consider Experiment CF-2 where the permeate flux was 0.5% that of the total flow. If this membrane thickness were decreased to 0.005mm and 0.0005 mm, the permeate fluxes would then be 4.5% and 44% respectively. Permeate flux rates such as these rival synthetic membrane efficiencies. Effective clay membranes have been made that are as thin as 12 μ m or less (Fritz and Eady, 1985). Future experiments will focus on producing significantly thinner clay membranes in the experimental cell.

Summary and Conclusions

The total pumping rate is not critical in achieving optimum solute rejection rates. Due to dispersion in the porous frit used adjacent to the membrane, the CPL seems to be completely (or nearly completely) destroyed at low flow rates. This observation suggests that clay membranes used with porous frit material may reach optimum rejection rates at lower pumping rates than those required for use with synthetic membranes.

The solute rejection efficiency decreases with increasing solution concentration. For the membranes and experiments reported here, the rejection efficiency ranged from 71% with 0.01 M NaCl solution down to 12% with 2.3 M NaCl solution. For more compacted clay membranes, solute rejection efficiencies should be higher.

There was an increase in required pumping pressure with increasing solute concentration. However, the relationship is poorly defined. Obviously, pressure and solution concentration are not the only variables. The required pressures fall within to well below the range required by synthetic membranes to perform similar separations.

The clay membranes we used were thick (approximately 0.5 mm). The active layer of most synthetic membranes is only 0.04 μm (0.00004 mm), approximately 1250 times thinner than the clay membranes used in these experiments. Yet clay membranes as this as 12 μm have been constructed (Fritz and Eady, 1985). Since Darcy's law states that the flow through a material of constant permeability is inversely proportional to its thickness, then, based on these experimental observations, a very thin clay membrane would be expected to have much higher flow rates than the ones used in these experiments. Future experiments will focus on testing very thin clay membranes.

The membranes generally exhibited reasonable stable rejection rates over time for chloride for a range of concentrations between 0.01 and 2.5 M. One membrane ran in excess of three months with no apparent loss of usability. This suggests that clay membranes may have a long life.

SOLUTE PRECIPITATION EXPERIMENTS

Objectives

The objectives of the experiments described in this section are to test the ability of clay membranes to precipitate sodium chloride (NaCl). Sodium chloride is the most common constituent of saline waters and is the only constituent of natural waters in which concentrations commonly exceed 20,000 mg/l (Feth, 1970). If a reverse osmosis waste reduction system is to be widely applicable to produced waters, it must be able to precipitate highly soluble dissolved minerals such as sodium chloride as well as less soluble dissolved minerals.

Previous Work

In conventional reverse osmosis, mineral precipitation is simply regarded as a problem that plugs membranes and limits their useful life (Mitsoyannis and Saravacos, 1977). Only two patents related to membrane-induced precipitation have been granted to date. Number 5,403,490 was issued to Satish Desai in 1995. His method uses a conventional cross-flow reverse osmosis system to concentrate metals to saturation and thus cause them to precipitate. Desai's system has several major drawbacks including fouling of the membrane in the conventional reverse osmosis unit by metal precipitates, and when used with high efficiency synthetic membranes, his system is incapable of precipitating any but slightly soluble compounds due to the high osmotic pressures generated. Patent Number 6,241,892 was issued to the New Mexico Tech Research Foundation in May 2001. This patent is the basis for the experimental work described in this section and describes the use of hyperfiltration-induced solute precipitation to desalt reverse osmosis waste streams.

Previous work by Fritz and Eady (1985) hyperfiltrated undersaturated calcium carbonate solutions through montmorillonite membranes and precipitated calcite. They concluded that the method might precipitate low solubility minerals. Later, Whitworth and DeRosa (1997) hyperfiltrated undersaturated metal chloride and metal carbonate solutions through montmorillonite membranes and precipitated CuCO_3 , CuCl_2 , CoCl_2 , and PbCl_2 .

Theoretical Experiments

To set up the theoretical experiments, we first needed to ascertain the necessary mathematics. Kedem and Katchalsky (1962) derived two equations which describe the flow of solution and solute through membranes. These equations were developed for non-electrolytes, but have been successfully applied to electrolytes (Spiegler and Kedem 1966; Harris *et al.* 1976; Mariñas and Selleck 1992; Whitworth *et al.* 1994). They describe a conservative, single solute system. The two equations are:

$$J_v = L_p (\Delta P - \sigma \Delta \pi) \quad (1)$$

and

$$J_s = \bar{c}_s (1 - \sigma) J_v + \omega \Delta \pi \quad (2)$$

where J_v = solution flux (cm/s) through the membrane, L_p = water permeation coefficient ($\text{cm}^3/\text{dyne}\cdot\text{s}$), ΔP = pressure difference across the membrane (dyne/cm^2), σ = reflection coefficient (dimensionless), $\Delta \pi$ = theoretical osmotic pressure difference across the membrane (dyne/cm^2), J_s = solute flux ($\text{mole}/\text{cm}^2\cdot\text{s}$) through the membrane, ω = solute permeation coeffi-

cient (mole/dyne·s), and \bar{c}_s = average solute concentration across the membrane in mole/cm³ where

$$\bar{c}_s = \frac{c_o + c_e}{2} \quad (3)$$

where c_o = concentration at the high-pressure membrane face (mole/cm³) and c_e = effluent concentration (mole/cm³).

The equation for $\Delta\pi$ for a dilute single solute is

$$\Delta\pi = vRT(c_o - c_e) \quad (4)$$

Where v is a factor that corrects for the number of particles due to ion formation. For example, since NaCl forms two ions in solution, Na^+ and Cl^- , then for NaCl, $v = 2$. However, for CaCl_2 , which forms one Ca^{++} ion and two Cl^- ions for each molecule of CaCl_2 , $v = 3$. In Equation 3, R is the gas constant (8.314×10^7 dyne·cm/mole·°K) and T is the temperature in °K.

Fritz (1986) suggested that three of the phenomenological coefficients of Kedem and Katchalsky (1962)— σ , ω , and L_p —are useful in describing the behavior of non-ideal, clay membrane systems. First, consider the reflection coefficient σ . Permissible values of σ range from zero to one. If $\sigma = 0$, then there is no membrane effect. In this case Equation 1 reduces to a one-dimensional form of Darcy's Law. If $\sigma = 1$, the membrane is ideal and no solute can pass. The value of σ for non-ideal clay membranes must be greater than zero, but less than one. Fritz and Marine (1983) calculated values of σ for a series of six experiments using montmorillonite clay membranes compacted to different porosities and NaCl solutions. The values of σ they determined ranged from 0.04 to 0.89. Fritz and Marine (1983) state that σ is important because it is a measure of osmotic efficiency. Thus, a membrane with a $\sigma = 0.90$ would exhibit 90% of the theoretically predicted osmotic pressure. For solutes such as NaCl, with identical anion and cation concentrations, $\sigma_{\text{anion}} = \sigma_{\text{cation}}$. However, for systems such as CuCl_2 , where the dissolved anion concentration is twice that of the cation concentration, the anion and the cation have differing values of σ .

The solute permeation coefficient ω describes the diffusion of solute through the membrane. For ideal membranes, $\omega = 0$ and no solute can pass through the membrane. For typically non-ideal clay membranes ω should be greater than zero. Elrick et al. (1976) measured ω for a Na-montmorillonite slurry with 90 % porosity and obtained a value of 3×10^{-15} mole/dyne·s. Fritz and Marine (1983) suggested that for more compacted clays, the value of ω should be considerably lower than 3×10^{-15} mole/dyne·s. For systems where the anion concentration is not equal to the cation concentration, $\omega_{\text{anion}} \neq \omega_{\text{cation}}$.

The water permeation coefficient L_p is related to the hydraulic conductivity K (in cm/s) by the expression (Fritz 1986)

$$L_p = \frac{K}{\rho g \Delta x} \quad (5)$$

where ρ is the fluid density in g/cm³, g is the gravitational constant in cm/s², and Δx is the membrane thickness in cm. In general, as L_p decreases, membrane efficiency increases (Fritz, 1986).

Fritz and Marine (1983) derived a steady-state solution that describes the concentration profile within the free solution abutting the membrane. Their equation is

$$c_x = (c_o - c_i) \left[\exp\left(\frac{-J_v x}{D}\right) - \exp\left(\frac{-J_v x_i}{D}\right) \right] + c_i \quad (6)$$

where c_x is the concentration in moles/cm³ at distance x (cm) from the membrane, and x_i is the distance from the membrane where $c_x = c_i$. In Equation 6, J_v represents the flux toward the membrane. Fritz and Whitworth (1994) state that the term $-\exp(-J_v x_i/D)$ in Equation 6 can be ignored if the length of the test cell is large relative to the ratio D/J_v .

Derivation

In order to use Equation 6 to model the proposed experiments, c_o must be known. An analytical expression for c_o can be derived by substituting in Equations 3, 4, 5, the following expression for ω

$$\omega = \frac{D}{RT\Delta x \zeta} \quad (7)$$

(where ζ is the tortuosity, defined here as the ratio of the actual path length through the membrane to the membrane thickness) and the steady-state relationships $J_s = J_v c_e$, and $c_i = c_e$, into Equation 2. This expression is

$$c_o = -c_i \cdot \frac{J_v \Delta x \zeta (1 + \sigma) + 2Dv}{J_v \Delta x \zeta (\sigma - 1) - 2Dv} \quad (8)$$

and is suitable for free solution.

Under what experimental conditions will NaCl precipitate from an initially undersaturated solution when it is passed through a clay membrane? Obviously, the value of c_o must reach or exceed saturation for NaCl. We can use Equation 8 to predict what the maximum value of c_o will be for a given set of experimental conditions, and Equation 6 to predict the concentration profile in the CPL in the free solution of the experimental cell.

First, consider an experiment with a clay membrane having a σ of only 0.075. The other experimental parameters are $J_v = 4.88 \times 10^{-5}$ cm/s (which translates to a flow rate of 3 ml/hr through a small, 1-in. diameter experimental cell), $c_i = 6.0$ molar, and $\Delta x = 0.15$ cm. Tortuosity = 7.0 (Barone et al. 1990, 1992), D of NaCl = 1.45×10^{-5} cm²/s, and $v = 2$. Using Equation 8, we find that $c_o = 6.44$ molar. This is above solubility for NaCl (≈ 6.2 molar) so precipitation should occur at the membrane face in this experiment. The concentration profile in the experimental cell, as calculated from Equation 6, shows that the CPL width is almost 2 cm, and that saturation is exceeded for a distance of approximately 0.22 cm from the membrane (Fig. 25).

One important aspect of these experiments is the effective osmotic pressure ($\sigma\Delta\pi$) because it must be overcome for flow to occur through the membrane. In this experiment, $\sigma\Delta\pi$ equals only 24 psi. This is because the effective osmotic pressure is a function of the difference in solute concentrations on either side of the membrane (See Eqns. 4 and 1) times the reflection

coefficient exceeded for a distance of 0.22 cm away from the membrane. Precipitation of NaCl should occur in the portion of the CPL where saturation is reached or exceeded.

If σ is higher than 0.075, then greater pressures will be required to force solution through the membrane. For comparison, consider a theoretical experiment in which $\sigma = 0.4$, and $c_i = 5.8$ molar, with all other parameters remaining the same (Fig. 26). Here we see that the maximum NaCl concentration reaches 8.5 molar (solubility ≈ 6.2 molar) at the membrane face and that saturation is reached or exceeded for a distance of 0.58 cm away from the membrane. The effective osmotic pressure ($\sigma\Delta\pi$) developed in this experiment is 770 psi. Therefore, even this scenario is achievable for typical reverse osmosis systems operating at pressures of 1000 to 1200 psi.

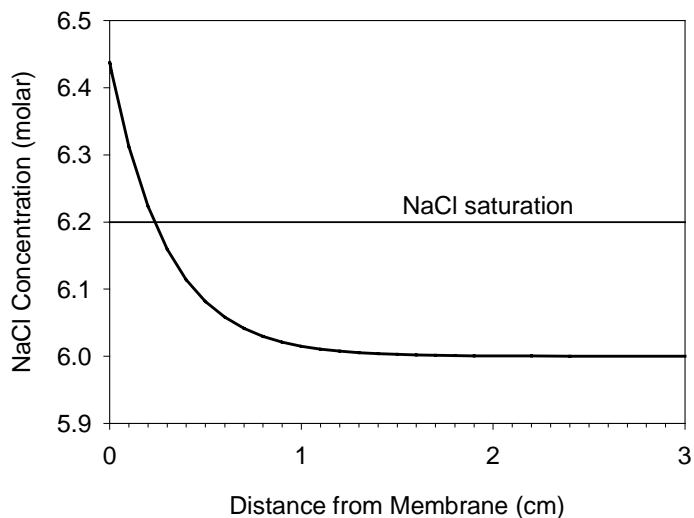


Figure 25. Graph of theoretical results for scenario where $\sigma = 0.075$ for a 6.0 molar NaCl solution hyperfiltrated through a montmorillonite membrane. Notice that the maximum concentration developed at the membrane face (c_o) exceeds the saturation value of 6.2 molar and that saturation is reached or exceeded for a distance of about 0.3 cm away from the membrane.

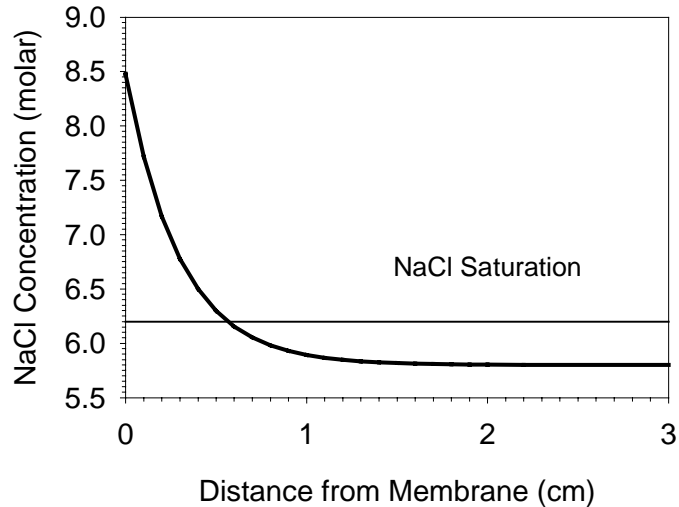


Figure 26. Graph of theoretical results for the second scenario where $\sigma = 0.2$ for a 5.8 molar NaCl solution hyperfiltrated through a montmorillonite membrane. Notice that the maximum concentration developed at the membrane face (c_o) exceeds the saturation value of 6.2 molar and that saturation is reached or exceeded for a distance of 0.58 cm away from the membrane. Precipitation of NaCl should occur in the CPL where saturation is reached or exceeded.

Precipitation of NaCl at reasonable pressures is dependent upon the membrane having a sufficiently low osmotic efficiency. How then is this low efficiency assured in the experimental membranes? Marine and Fritz (1981) derived a model for calculating values of σ by arguing that under stationary conditions, the thermodynamic forces acting across the membrane are counterbalanced by the sum of mechanical frictional forces operating on the solution components within the membrane. Their equation is

$$\sigma = 1 - \frac{\left[\left(\frac{f_{cw}}{f_{aw}} \right) + 1 \right] K_s}{\left\{ \left[\left(\frac{f_{cw}}{f_{aw}} \right) \left(\frac{\bar{C}_a}{\bar{C}_c} \right) + 1 \right] + \left(\frac{f_{am}}{f_{aw}} \right) \left(\frac{f_{cm}}{f_{am}} \right) \left(\frac{\bar{C}_a}{\bar{C}_c} \right) + 1 \right\} \phi_w} \quad (9)$$

where f_{ij} is the frictional coefficient between one mole of component i and an infinite amount of component j in dyne seconds per centimeter per mole, c refers to the cation, a refers to the anion, w refers to water, \bar{C}_i is the average concentration of component i across the membrane in dynes per mole, and ϕ_w refers to the water content of the membrane, which is equivalent to the porosity.

Marine and Fritz (1981) used Equation 9 to model the relationship between porosity and values σ for various NaCl concentrations for montmorillonite membranes (Fig. 27). Their model shows that values of σ between 0.4 and 0.1 should be expected for a 6.0 molar NaCl solution at membrane porosities of between 58 and 73%. Previous experiments (Whitworth and DeRosa 1997) suggest that membrane porosities in this range are not easily obtainable by hydraulic compaction during membrane sedimentation alone. Therefore, it will be necessary to physically compact the membranes used in these experiments to the required porosities. Whitworth and Fritz (1994) compacted two montmorillonite membranes to porosities of 44.8 and 62.0 % using a 20-ton hydraulic press.

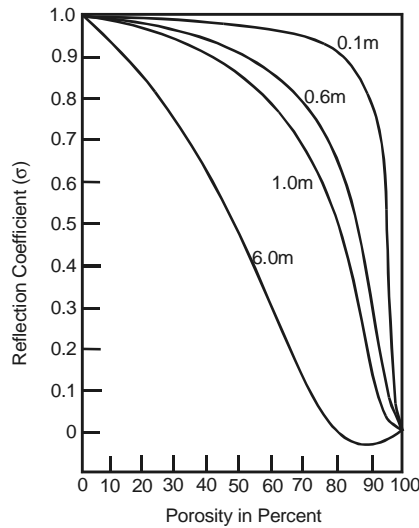


Figure 27. Graph derived from Equation 9 showing relationship between the reflection coefficient and porosity for montmorillonite (smectite) membranes for differing molar concentrations of NaCl (Redrawn from Marine and Fritz 1983). Notice that for 6.0 molar NaCl, porosities between 73% and 58% will yield values of σ of 0.1 and 0.4, respectively.

Methods

Clay preparation

The clay used in these experiments was a commercially available kaolinite from ECC International (Quality China Clay). Kaolinite was chosen for these experiments because it does not swell when exposed to water. In previous experiments, when bentonite clay was used, it swelled and bent the 316 stainless steel frit that had been placed above the clay membrane (Whitworth and Gu, 2001).

The first step in preparation of the kaolinite clay for use in the experiments was to separate the 0.2 μm and smaller size fraction. This was done using standard sedimentation techniques. Following size separation, the clay was freeze-dried using a Model 4.5 Labconco bench-top freeze dryer. The method used was that reported by Whitworth and Fritz (1994). After freeze-drying, the clay is stored in nested, tightly sealed ziplock bags to prevent moisture from contacting the clay. The purpose of freeze-drying is to remove the moisture content of the clay

which allows density determinations. Vacuum freeze-drying removes non-adsorbed water (Zimmie and Almaleh, 1976, Fritz and Marine, 1983).

Experimental cell and flow configuration

An experimental cell was constructed of 316 stainless steel and was designed to operate at pressures up to 3000 psi (Figure 28). This cell used perforated flow distribution disks (not shown) in the top of the cell above the solution reservoir and below the 316 stainless steel frit immediately below the membrane to promote uniform flow in the experimental cell. The cell was connected to an Isco syringe pump (Model 500D) capable of maintaining constant flow rates ($\pm 0.01\%$) at pressures up to 3750 psi (Figures 29 and 30).

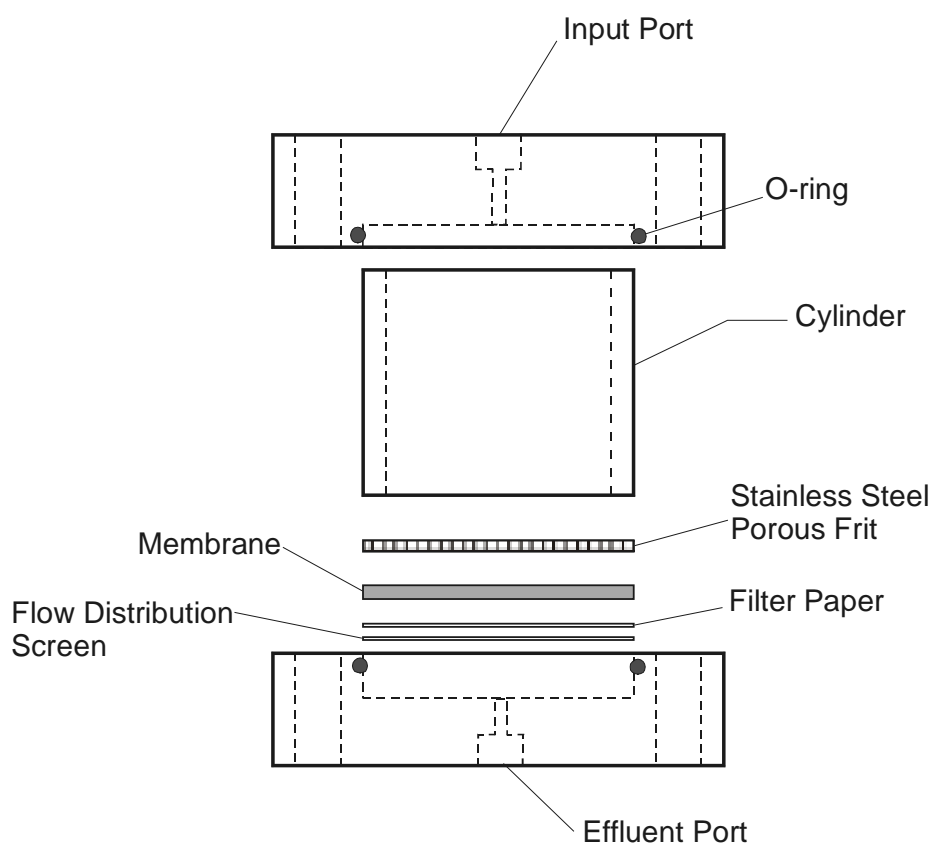


Figure 28. Experimental cell for precipitation experiments. The entire assembly is locked in place with nuts on threaded rods that pass through the holes near the edges of the top and bottom plates. Since all cell dimensions are known to ± 0.001 inches, the membrane thickness can be calculated from the measured distance between the inside surfaces of the outer plates. Cylinders of differing lengths can be used depending upon CPL length for a given experiment.

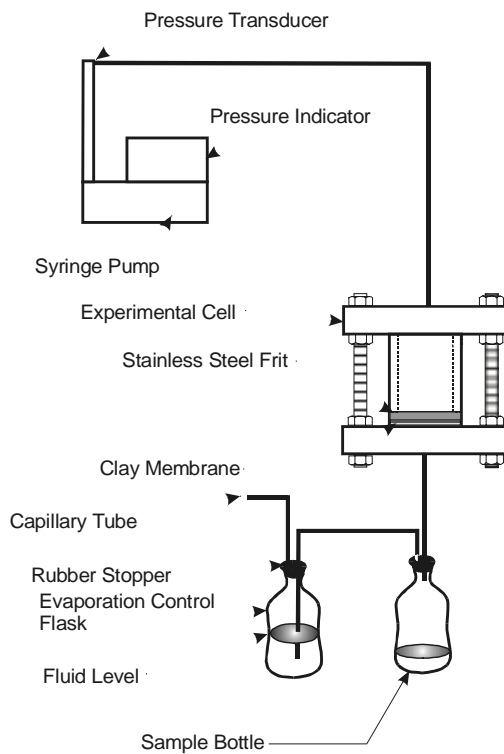


Figure 29. Experimental setup for hyperfiltration experiments.

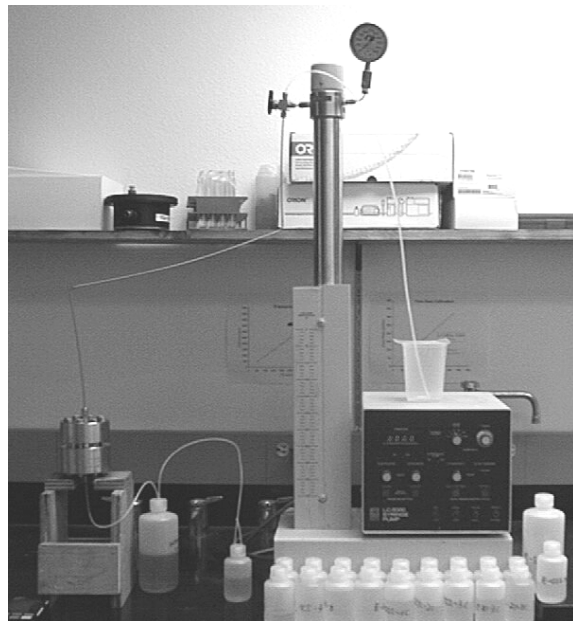


Figure 30. Photograph of precipitation experiment. Note that the collection bottle attached to the cell is larger than the ones used in front of the pump and the dark color of the liquid in the bottle. This sample bottle is collecting WD-40 that is being run through the cell to displace the water in the cell in Experiment H-19.

Procedure for preparing the membrane

1. Connect outlet fitting to bottom endcap of CPL cell.
2. Place bottom endcap on CPL stand.
3. Connect flexible tube from fitting to collection bottle.
4. Place top distribution plate into the bottom endcap. The top distribution plate is thinner than the bottom distribution plate and is used to create a larger volume to hold the slurry.
5. Place the stainless steel frit into the bottom endcap.
6. Place #2 Whatman filter paper into the bottom endcap.
7. Place 0.05 µm Millipore filter paper into the bottom endcap.
8. Measure on a scale a small amount of freeze-dried clay (about 1g). Place clay in small beaker.
9. Add DI water (about 16 ml) to the clay, stir with a magnetic stirrer for 5 minutes.
10. When stirring is complete, remove stirrer with tweezers and rinse tweezers and stirrer with DI water into a collection bottle. Any clay that sticks to the magnetic stirrer or tweezers will be measured afterward to precisely calculate the amount of clay in the membrane.
11. Pour the slurry into the bottom endcap. Let settle for 12 hours.
12. Remove outlet fitting from the bottom endcap.
13. Place bolt through the center fitting hole in the endcap. Use bolt to push the distributor plate up until the membrane assembly is just outside the endcap. Use small spatula to remove the membrane assembly.
14. Place membrane assembly on bottom part of die. Place 0.05 µm Millipore filter and Whatman #2 filter paper on top of the membrane. Place middle part and then top part of die on top of the bottom part.
15. Rinse the bottom endcap, frit, outlet fitting, flexible tube, and distribution plate with DI water into collection bottle to collect any remaining clay.
16. Press die in hydraulic press in incremental pressures; for each 1000-pound increment, let the die sit for 20 minutes before increasing the pressure.
17. When the hydraulic pressure reaches 50,000 pounds, let sit for four hours.
18. Remove the die from the press and remove the membrane assembly. Use calipers to measure the thickness of the membrane assembly. Take at least six measurements at various locations on the membrane assembly.
19. Hold the membrane assembly up to a light to observe any damage to the membrane or unevenly distributed clay. Make note of any abnormalities. If the membrane is damaged, discard it and make another membrane.

Procedure for assembling the experimental cell

1. Insert bottom flow distributor into the bottom endcap of cell.
2. Insert steel frit into the bottom endcap.
3. Insert membrane assembly into the bottom endcap.
4. Insert rubber O-ring into the groove of the bottom endcap.
5. Insert CPL cylinder into the bottom endcap.
6. Place top flow distributor on top of CPL cylinder.

7. Insert O-ring into top endcap.
8. Place top endcap onto CPL cylinder. Use press to gently bring the two halves together.
9. Bolt the CPL cell together using bolts through the ring of holes in the endcaps.
10. Connect the outlet fitting to the bottom endcap.

Procedure for setting up the experiment

1. Fill the syringe pump with deionized water. It might be necessary to purge and refill the pump several times to ensure that no air is trapped in the pump.
2. Place the CPL cell on the stand and connect the flexible tube to the outlet fitting.
3. Fill the inside of the cell with deionized water using a small syringe.
4. Attach the inlet fitting to the top endcap and make sure no air is in the cell.
5. Weigh a sample bottle. Use a marker to put the weight and number of the bottle on the bottle.
6. Connect the flexible tube to the sample bottle connect the evaporation control bottle to the sample bottle.
7. Run the pump before attaching it to the cell on the “purge” setting until water comes from the line to be attached to the cell. Turn pump off and switch pump from “purge” to “pump”.
8. Connect the pump to the top of the cell inlet fitting.

Procedure for running the experiment

1. Adjust the flow rate of DI water through the pump until the pressure is at steady state at about 1000 psi.
2. Periodically remove the sample bottle and replace it with a new one. Weigh the sample bottle before and after it is attached to the cell.
3. When steady state is achieved, stop pumping. Do not rinse the pump until the pressure has gone down. It is important that the pressure not drop too quickly as this may cause damage to the membrane. Rinse the pump several times with NaCl solution.
4. Fill the pump with NaCl solution.
5. Run the pump at the same flow rate as before with the deionized water. If the pressure becomes to high, the flow rate may be decreased.
6. Repeat step 2.
7. Deactivate the pump. Do not detach the cell from the pump while the pressure is high.
8. Rinse the pump with deionized water.

Procedure for sample dilution

Since the solute concentration of many of the samples was in excess of what could be measured by the analytical instruments, dilution was often needed. Materials needed: Eppendorf Series 2100 pipette, pipette tips, DI water, 50 ml Pyrex flasks, Samples from CPL experiment, 30 ml sample bottles, squeeze bottle. The dilution procedure is as follows:

1. Preparing the pipette: Adjust the pipette to draw 1 ml of liquid. Firmly attach the pipette tip to the pipette.

2. Filling the tip: Remove the lid of a sample bottle from the CPL experiment. Press the control button on the top of the pipette to the first stop. Insert the pipette tip into the sample. Make sure to place the end of the tip far enough from the surface so that no air will get into the tip when drawing in liquid. Slowly let the bottom slide back to its original position. Remove the pipette from the sample.
3. Emptying the pipette tip: Remove the lid of a 50 ml volumetric flask. Empty the pipette tip into the volumetric flask by slowly depressing the top button to the first stop. Remove the last remaining liquid in the tip by quickly pressing the top button to the second stop.
4. Diluting the sample: Use the squeeze bottle to fill the 50 ml volumetric flask to the 50 ml fill mark with DI water. When the flask is nearly full to this mark, use single drops of DI water from the squeeze bottle to ensure accuracy in the dilution. Place the lid on the flask and mix by turning the flask upside down many times.
5. Filling the bottle: Remove the lid from a 30 ml bottle and pour 30 ml of diluted sample into the bottle. Securely fasten the lid onto the bottle and label appropriately with a marker.
6. Rinsing the volumetric flask: Empty the remaining liquid from the flask. Fill the volumetric flask with deionized water up to the 50 ml mark. Place the lid on the volumetric flask and mix using the same procedure from step 4. Rinse the flask three times with deionized water after each use.

Procedure for disassembling the cell

1. Remove the inlet fitting from the top of the cell.
2. Remove the bolts on the cell. To loosen the top and bottom endcaps, place four small nuts (two on each opposite side in the gap between the endcaps so that the nuts line up with the bolt holes.) Place two thin bolts through the bolt holes and thread them through the nuts. By turning the nuts with a wrench, the two endcaps can be loosened.
3. Separate the endcaps. The cylinder should stay with the bottom endcap. Remove the outlet fitting and place a bolt through the bottom hole to push the membrane assembly out of the endcap. Use a press to push on the bolt by placing a metal cylinder with a greater inside diameter than the outside diameter of the CPL cylinder. Place the larger cylinder around the CPL cylinder. The press will now push the cylinder out of the endcap.
4. Remove the O-ring from the bottom endcap with tweezers. Take care not to damage the membrane as it may now be close to or wedged against the O-ring.
5. Remove the membrane assembly with tweezers.
6. Place membrane assembly in a small container and seal it with laboratory film.

Exceptions to the standard procedures

Control experiments were run with no clay in the membrane assembly. The goal of the control experiments was to determine if the crystals found were formed by hyperfiltration-induced precipitation or by evaporation when the membrane was removed from the cell.

Experiment H-9, Experiment H-11, and Experiment H-19 had several significant changes to the procedures listed above. The goal of these experiments was to determine if a statistically

significant difference existed between the mass of NaCl crystals formed on filter paper in an experiment performed with no clay and filter paper from an experiment performed using a clay membrane. In order to accomplish this the following changes were made in the standard procedures:

1. Weigh the filter papers before membrane assembly. The mass of the crystals will be the difference in the weight between the weight measured in this step and the weight measured in the experiment.
2. Disassembling the cell: After step 4 of the standard procedures, use a syringe to slowly extract all of the water from the cell. Place syringe on the edge of the membrane assembly to minimize any damage this may cause and prevent the flow of salt crystals into the syringe.
3. Remove the membrane assembly: Separate the top Whatman filter paper and Millipore filter from the membrane assembly with tweezers. Place in small container and seal it with laboratory film.
4. Dry the filter paper. Weigh the top part of the membrane assembly just after removal from the cell. This weight is filter paper plus the precipitate, the clay stuck to the filter paper and the water left on and in the paper. Place the filter paper in a small open container on top of an upside-down 500-ml plastic beaker. Place a 1000-ml plastic beaker with holes punched in the sides on top. The reason for this is to evaporate the water from the filter paper while preventing contamination from any falling dust particles in the lab.
5. Weigh the dried filter paper. Once the filter paper is dry, weigh it again. This will measure the mass of the Whatman filter paper, the Millipore filter, the clay stuck to the Millipore filter, the salt from precipitation and the salt from evaporation. The clay that is stuck on the filter paper is then removed and the filter paper is weighed a third time.
Note that Experiment E-I was changed to a mass balance experiment while it was in the process of running and therefore the filter papers were not weighed before membrane assembly.

Experiment H-16 had a few significant changes to the standard procedures. The goal of this experiment was to observe the difference in the size, shape and amount of crystals that formed on top of the membrane assembly between an experiment with and without clay. While some changes were made in the procedure in pursuit of this goal, others were made to see what effect they would have on the performance of the experiment.

1. Use 0.1 N NaCl solutions instead of DI water while running the experiment.
2. Press the membrane assembly to 40,000 pounds instead of 50,000.
3. Place a frit on top of the membrane assembly.
4. Place a Teflon washer on top of the frit to stop solution from short-circuiting around the membrane assembly.
5. Observe the top frit under a microscope immediately after the disassembly of the cell to check for crystals before crystals can form from evaporation.

Experiment H-19 used WD-40 to displace the solution in the cell and in the membrane assembly, preserving the crystals that formed by precipitation. The goal of this experiment was to eliminate the possibility of evaporative crystals from forming by removing all of the solution from the cell before the cell was disassembled. A control experiment (H-20) was used to check for crystal formation without the presence of clay. A beaker test was run to see if WD-40 would

cause precipitation of NaCl from under saturated solution. The following deviations from standard procedures were used in Experiment H-19:

1. Weigh the filter papers before the preparation of the membrane assembly. This allows for an accurate measurement of the amount of clay in the membrane assembly by weighing the assembly after it is prepared.
2. During the membrane preparation let the slurry dry for 24 instead of 12 hours. This will ensure that the clay will be dry. Dry the membrane assembly in a dehydrator for 12 hours to remove all of the moisture and allow the mass of the clay to be properly determined.
3. Place a frit on top of the membrane assembly while assembling the cell.
4. After the NaCl solution has run through the cell, remove the solution and fill the pump with WD-40. Run WD-40 through the cell. Use at least 200 ml of WD-40 to ensure the displacement of all of the solution in the cell.
1. A beaker test was used to determine if WD-40 might cause precipitation of NaCl from under saturated solution by lowering the solubility of the salt. WD-40 displaces most of the water in the cell; some of the water is emulsified. No precipitation was observed.

Results

Twenty different experiments were either completed or attempted (Table 17). Perhaps the single-most difficult experimental problem is to displace the remaining brine from the experimental cell at the end of the experiment to prevent crystal formation by evaporation once the membrane is removed from the cell for examination. We tried several approaches. The first was the use of cooking oil to displace the water. However, our control experiment demonstrated this was not a reliable method. We then used Crown, a chemical designed for water displacement. Again, control experiments demonstrated that this approach was not suitable. Lastly we tried displacing the water with WD-40. This approach was by far the most successful and provided reasonable results. To save space in this report, we will only report in detail on six experiments; 1, 2, 3, 4, 19 and 20.

Table 17. Summary of Solute Precipitation Experiments

Experiment	Clay	Solution	Purpose	Displacement Chemical	Results
H-1	Kaolinite	90% saturated NaCl	Test precipitation of NaCl	Cooking oil	Yes-microprobe
H-2	Kaolinite	90% saturated	Test precipitation of NaCl	Cooking oil	Yes-microprobe
H-3	Kaolinite	NaCl	Test precipitation of NaCl	Cooking oil	Yes-microprobe
H-4	Kaolinite	90% saturated	Test precipitation of NaCl	Cooking oil	No
H-5	None	NaCl	Test ability of crown to displace water	Crown	Yes-microprobe
H-6	None	90% saturated	Test ability of crown to displace water-different technique	Crown	O-ring failure-no data
H-7	None	NaCl	Test ability of crown to displace water-different technique	Crown	Yes-microprobe
H-8	None	90% saturated	Test ability of vegetable oil to displace water	Cooking oil	Yes-visual inspection
H-9	Kaolinite	NaCl	Measure mass balance	None	Results inconclusive
H-10	Kaolinite	90% saturated	Measure mass balance	None	Membrane damaged during assembly—no data
H-11	Kaolinite	NaCl	Measure mass balance	None	Membrane failure-no data
H-12	Kaolinite	90% saturated	Measure mass balance	None	Cell leaking-no data
H-13	Kaolinite	NaCl	Measure mass balance	None	Cell did not hold pressure—no data
H-14	Kaolinite	90% saturated	Measure mass balance	None	Cell did not hold pressure—no data
H-15	Kaolinite	NaCl	Measure mass balance	None	Membrane failure-no data
H-16	Kaolinite	Use 0.1 M NaCl	Test precipitation of NaCl	None	No crystals observed
H-17	Kaolinite	90% saturated	Measure mass balance	WD-40	Crystals observed with light microscope Mass balance results inconclusive
H-18	None	NaCl	Blank	WD-40	Crystals observed with light microscope. Were less numerous than in the corresponding experiment (H-17) which was run using a clay membrane
H-19	Kaolinite	90% saturated	Test precipitation of NaCl	WD-40	Numerous groups of large crystals found with light microscope
H-20	None	NaCl	Blank for experiment 19	WD-40	Two crystals found on frit. Orders of magnitude fewer crystals observed in this blank than in experiment 19.

Experiment H-1 (Table 18) used a bentonite membrane compacted to 30,000 psi. The porosity of this membrane was 32%. We used cooking oil, which is light in weight, to displace the brine from the experimental cell at the end of the experiment. No crystals formed in our beaker tests when we poured brine into the oil or oil into the brine. After examination with the microprobe, we saw numerous NaCl crystals on the membrane (Figures 31, 32, and 33).

Table 18. Results for Experiment H-1

Sample Number	Δp (psi)	Cl- (moles/L)	J_v (cm/s)	Elapsed Time (hrs)	Comments
RC11-0	--	4.56	--	--	Stock Solution
RC11-1	937	0.45	1.10×10^{-5}	27.0	--
RC11-2	1098	0.96	1.10×10^{-5}	56.5	--
RC11-3	1138	1.56	1.10×10^{-5}	94.0	--
RC11-4	1203	2.19	1.10×10^{-5}	118.3	--
RC11-5	--	2.68	--	--	--



Figure 31. Electron micrograph of NaCl crystals present on the surface of the membrane of Experiment H-1

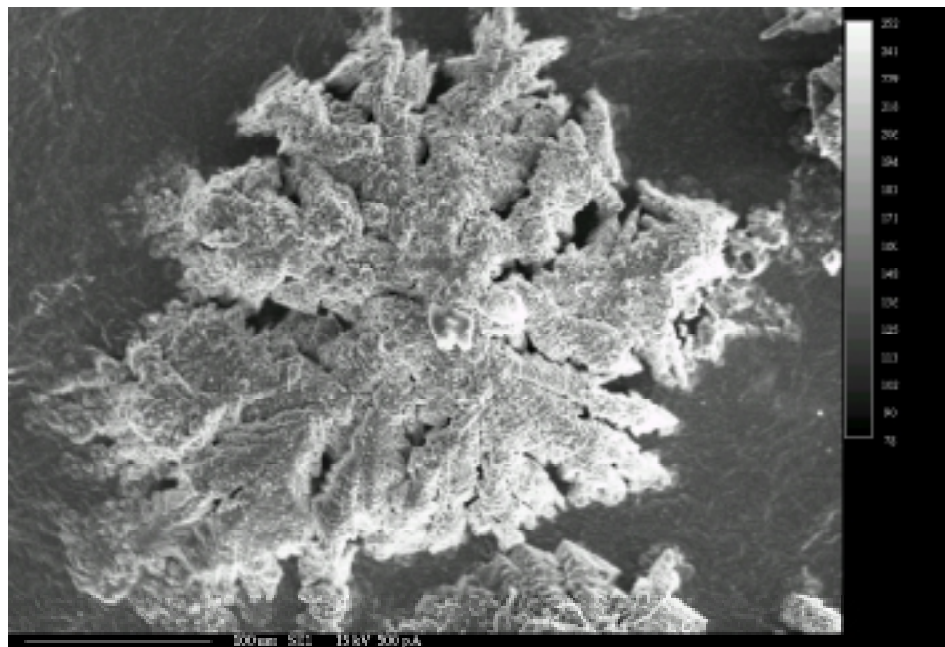


Figure 32. Enlargement of a single crystal cluster from Experiment H-1 shown in Figure 31.

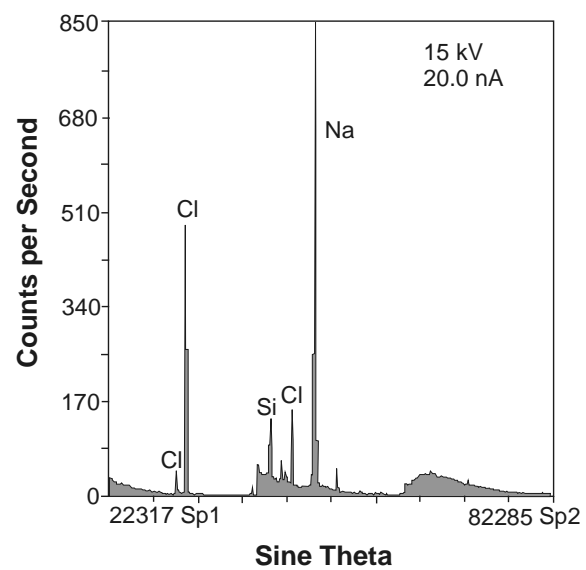


Figure 33. Energy-dispersive X-ray scan of crystals shown in Figures 31 and 32. The peaks in this scan confirm that the crystals shown in Figures 30 and 31 are composed of NaCl.

Experiment H-2 (Table 19) used a kaolinite membrane compacted to 50,000 psi with porosity of 30%. At the end of this experiment the brine remaining in the experimental cell was displaced with cooking oil. Subsequent examination on the microprobe showed the presence of NaCl crystals (Figures 34 and 35).

Table 19. Results for Experiment H-2

Sample Number	Δp (psi)	Cl- (moles/L)	J_v (cm/s)	Elapsed Time (hrs)	Comments
RC12-0	--	4.63	1.10×10^{-3}	--	Stock Solution
RC12-1	346	0.32	1.10×10^{-3}	0.27	--
RC12-2	377	1.10	1.10×10^{-3}	0.57	--
RC12-3	422	1.87	1.10×10^{-3}	1.02	--
RC12-4	466	2.79	1.10×10^{-3}	1.55	--
RC12-5	508	3.42	1.10×10^{-3}	2.22	--
RC12-6	555	4.02	1.10×10^{-3}	3.78	--
RC12-7	563	4.35	1.10×10^{-3}	4.23	--
RC12-8	573	4.44	1.10×10^{-3}	5.23	--
RC12-9	583	4.46	1.10×10^{-3}	6.75	--
RC13-10	583	4.52	1.10×10^{-3}	9.52	--
RC12-11	579	4.51	1.10×10^{-3}	11.8	--
RC12-12	589	4.54	1.10×10^{-3}	24.4	--
RC12-13	--	4.54	1.10×10^{-3}	29.5	--
RC12-14	543	4.52	1.10×10^{-3}	33.0	--
RC12-15	541	4.52	1.10×10^{-3}	36.0	--
RC12-16	552	4.57	1.10×10^{-3}	47.2	--
RC12-17	534	4.54	1.10×10^{-3}	53.0	--
RC12-18	535	4.62	1.10×10^{-3}	58.1	--
RC12-19	542	4.59	1.10×10^{-3}	69.7	--
RC12-20	542	4.58	1.10×10^{-3}	71.6	--
RC12-21	531	4.58	1.10×10^{-3}	75.3	--
RC12-22	531	4.58	1.10×10^{-3}	81.7	--
RC12-23	539	4.59	1.10×10^{-3}	94.5	--
RC12-24	530	4.59	1.10×10^{-3}	100.8	--
RC12-25	524	4.52	1.10×10^{-3}	105.8	--
RC12-26	540	4.66	1.10×10^{-3}	118.1	--
RC12-27	543	4.65	1.10×10^{-3}	123.0	--
RC12-28	--	4.59	--	--	Pump Solution

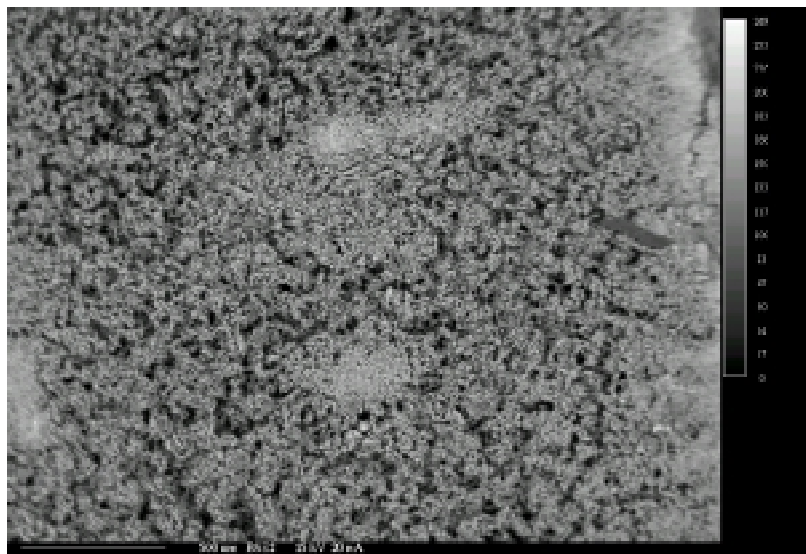


Figure 34. Microprobe scan showing distribution of NaCl crystals across surface of kaolinite membrane from Experiment H-2. The NaCl is the bright white part of the scan. The brine remaining in the experimental cell was displaced with cooking oil before the cell was disassembled.

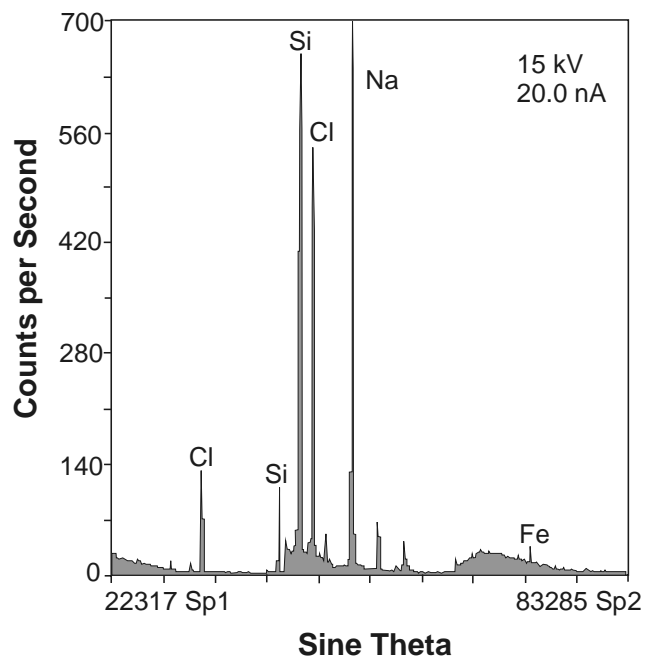


Figure 35. Energy-dispersive X-ray scan of crystals shown in Figure 34. The peaks in this scan confirm that the crystals are composed of NaCl. This scan is of the white area in Figure 13.

Experiment H-3 (Table 20) used a kaolinite membrane compacted to 50,000 psi. The porosity of this membrane was 37.1%. Again, at the end of the experiment, the brine remaining in the experimental cell was displaced with cooking oil. The membrane was then examined on the microprobe. Figures 36 and 37 show examples of the crystals observed.

Table 20. Results for Experiment H-3

Sample Number	Δp (psi)	Cl- (moles/L)	J_v (cm/s)	Elapsed Time (hrs)	Comments
RC13-0	--	4.82	--	--	Stock Solution
RC13-1	572	0.68	9.86×10^{-4}	0.35	--
RC13-2	612	1.16	9.86×10^{-4}	0.67	--
RC13-3	668	1.74	9.86×10^{-4}	1.02	--
RC13-4	724	2.36	9.86×10^{-4}	1.35	--
RC13-5	777	2.87	9.86×10^{-4}	1.70	--
RC13-6	823	3.29	9.86×10^{-4}	2.03	--
RC13-7	862	3.61	9.86×10^{-4}	2.37	--
RC13-8	901	3.86	9.86×10^{-4}	2.70	--
RC13-9	931	4.15	9.86×10^{-4}	3.03	--
RC13-10	971	4.26	9.86×10^{-4}	3.65	--
RC13-11	1006	4.30	9.86×10^{-4}	4.23	--
RC13-12	1031	4.56	9.86×10^{-4}	4.73	--
RC13-13	1068	4.61	9.86×10^{-4}	5.58	--
RC13-14	1082	4.76	9.86×10^{-4}	6.75	--
RC13-15	1099	4.81	9.86×10^{-4}	8.42	--
RC13-16	1107	4.79	9.86×10^{-4}	11.48	--
RC13-17	1128	4.73	9.86×10^{-4}	20.77	--
RC13-18	1134	4.80	9.86×10^{-4}	25.48	--
RC13-19	1053	4.72	9.86×10^{-4}	29.87	--
RC13-20	1076	4.81	9.86×10^{-4}	34.50	--
RC13-21	1072	4.77	9.86×10^{-4}	45.33	--
RC13-22	1076	4.71	9.86×10^{-4}	51.95	--
RC13-23	1055	4.78	9.86×10^{-4}	57.83	--
RC13-24	1042	4.81	9.86×10^{-4}	69.03	--
RC13-25	1055	4.37	9.86×10^{-4}	79.15	--
RC13-26	1031	4.88	9.86×10^{-4}	94.93	--
RC13-27	1009	4.79	9.86×10^{-4}	100.37	--
RC13-28	--	4.81	--	--	Pump Solution

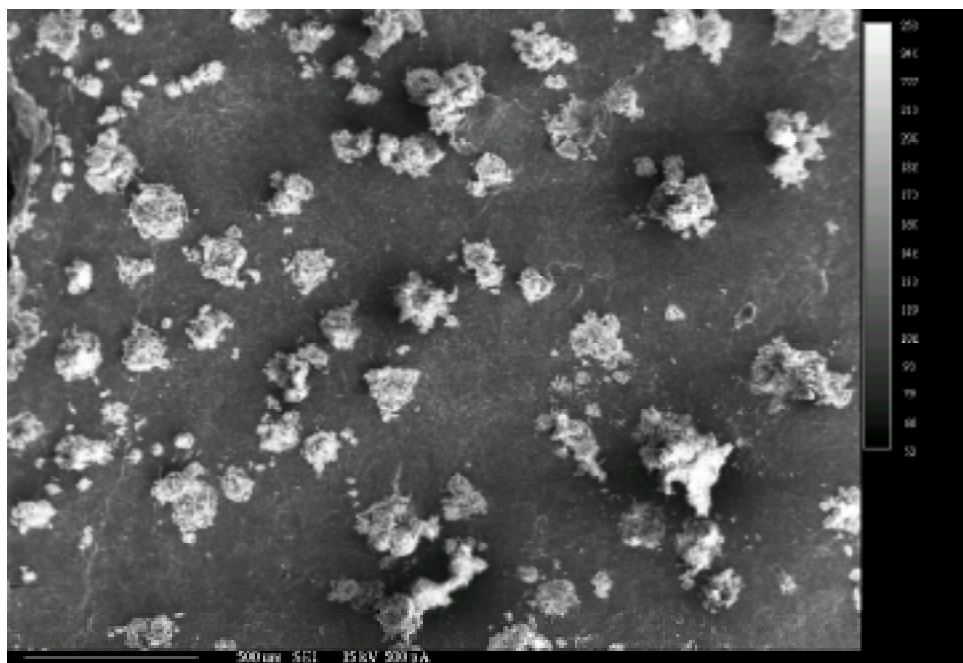


Figure 36. Microprobe scan showing distribution of NaCl crystals across surface of kaolinite membrane from Experiment H-3. The brine remaining in the experimental cell was displaced with cooking oil before the cell was disassembled

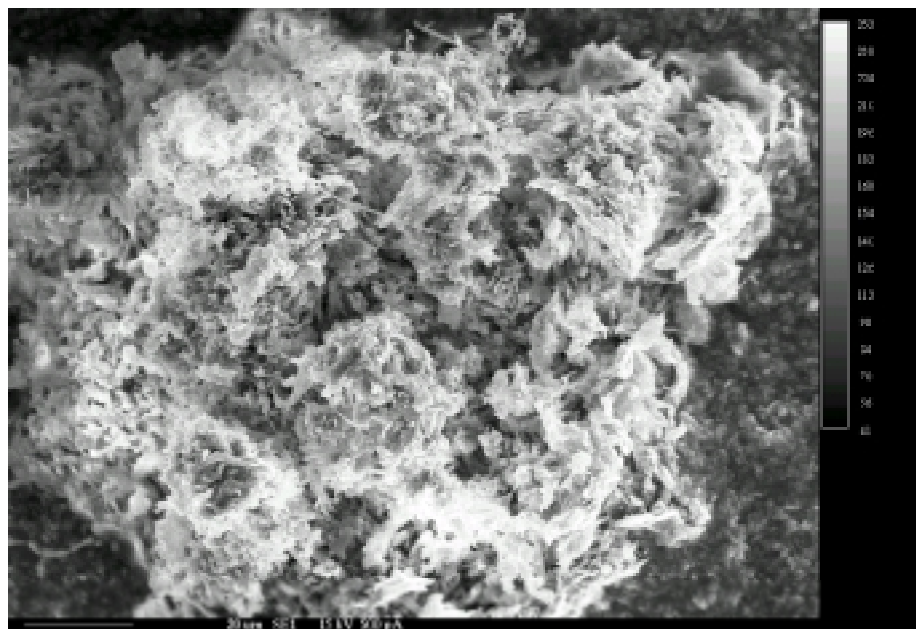


Figure 37. Close-up of one of the crystal clusters shown in Figure 35.

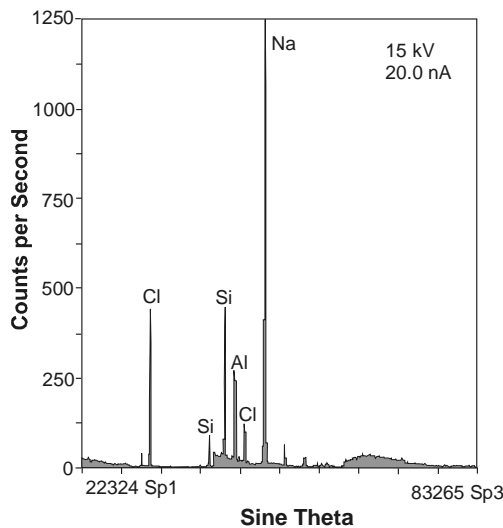


Figure 38. Energy dispersive X-ray scan of crystals shown in Figures 36 and 37. The peaks in this scan confirm that the crystals are composed of NaCl.

Experiment H-4 (Table 21) used a bentonite membrane compacted to 30,000 psi. The porosity of this membrane was 44.0%. At the end of the experiment, the brine remaining in the experimental cell was displaced with light weight cooking oil. The membrane was then examined on the microprobe. No NaCl crystals were observed when this membrane was examined on the microprobe. However, Figure 39 shows some unidentified crystals that were observed.

Table 21. Results for Experiment H-4

Sample Number	Δp (psi)	Cl- (M)	J_v (cm/s)	Elapsed Time (hrs)	Comments
RC14-0	--	4.90	--	--	Stock Solution
RC14-1	130	0.52	1.10×10^{-4}	2.17	--
RC14-2	388	0.90	1.64×10^{-4}	4.08	--
RC14-3	429	1.55	1.64×10^{-4}	6.37	--
RC14-4	488	2.40	1.64×10^{-4}	10.05	--
RC14-5	601	3.77	1.64×10^{-4}	22.03	--
RC14-6	615	4.44	1.64×10^{-4}	24.57	--
RC14-7	640	4.63	1.64×10^{-4}	33.75	--
RC14-8	639	4.79	1.64×10^{-4}	47.67	--
RC14-9	678	4.85	1.64×10^{-4}	68.25	--
RC14-10	748	4.94	1.64×10^{-4}	92.88	--
RC14-11	790	4.92	1.64×10^{-4}	118.50	--
RC14-12	785	4.85	1.64×10^{-4}	139.63	--
RC14-13	795	4.83	1.64×10^{-4}	166.00	--

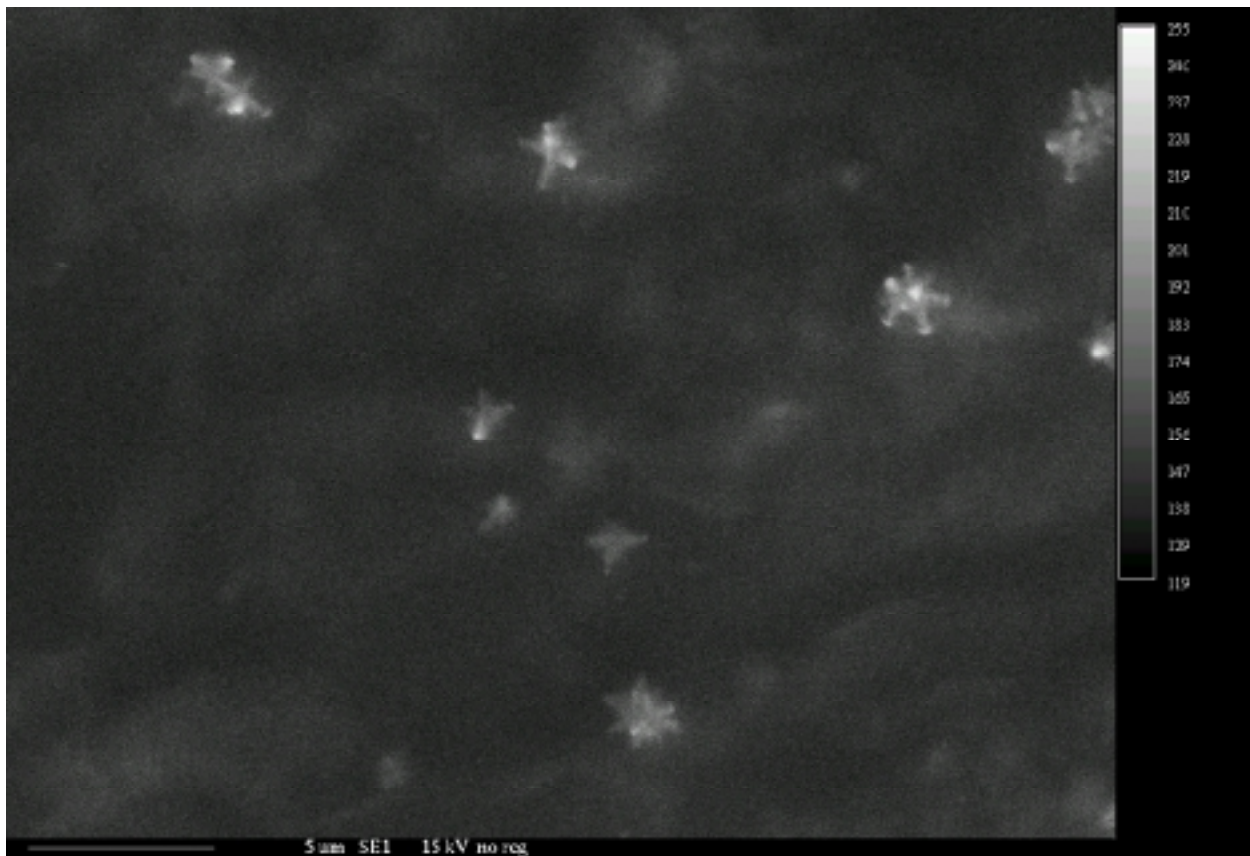


Figure 39. Electron micrograph of unknown crystals on surface of membrane from Experiment H-4. These crystals do not do not behave like NaCl crystals. No energy-dispersive X-ray scan is available for these crystals. Their composition is unknown. No similar crystals were observed on any of the other membranes.

Experiment H-19 (Table 22) used WD-40 to displace the remaining brine at the end of the experiment and used a dry compaction technique to form the kaolinite membrane. The 0.87 grams of freeze-dried kaolinite used to construct the membrane were compacted to 50,000 lbs of total force. The data from the control experiment (Experiment H-20) is shown in Table 23. Crystals were photographed in abundance on the frit after the clay experiment (Experiment 19) was run while only two crystals could be found after the control (Experiment 20). To accomplish this goal, photographs were taken of the top frit in both the clay and control experiments. The photographs were taken using a camera attached to a light microscope set on X18 power. The width of the photographs is equivalent to 2 mm. Figures 40 and 41 are of the frit from the clay experiment, Figure 42 is of the frit from the control experiment.

Table 22. Data for Experiment H-19

Sample Number	Δp (psi)	Cl- (M)	J_V (cm/s)	Elapsed Time (hrs)	Comments
SS	NA	0.00	NA	NA	Stock Solution
1	210	0.00	.824	3.40	--
2	760	0.00	3.65	14.43	--
3	690	0.00	3.65	22.12	--
4	640	0.00	3.65	29.05	--
5	600	4.43	3.65	35.28	--
6	790	4.68	3.65	39.22	--
7	990	4.35	3.65	43.73	--
8	1070	3.94	3.65	52.60	--
9	1150	4.51	3.65	58.15	--
10	750	4.43	3.65	66.78	--
11	1080	4.39	3.65	72.45	--
12	810	4.70	3.65	79.20	--
13	1010	4.71	3.65	84.48	--

Table 23. Data for Control Experiment H-20

Sample	Elapsed Time min	Effluent Concentration of Cl- ppm	Volume ml	J_V $\text{cm}^3/\text{cm}^2\text{s}10^{-4}$
Stock Solution	NA	167350	NA	NA
1	204	99	11.5	.824
2	866	80	165.5	3.65
3	1327	82	115.25	3.65
4	1743	77	104	3.65
5	2117	157150	93.5	3.65
6	2353	165800	59	3.65
7	2624	154200	67.75	3.65
8	3156	139850	133	3.65
9	3489	160000	83.25	3.65
10	4007	156900	129.5	3.65
11	4347	155700	85	3.65
12	4752	166650	101.25	3.65
13	5069	166850	79.25	3.65

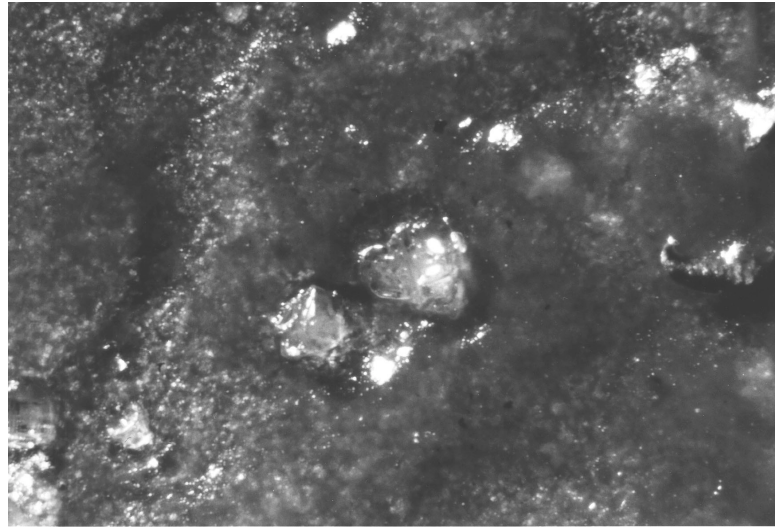


Figure 40. Photograph taken near the center of the frit in Experiment H-19. Two large crystals are visible in the center of the picture. The crystals are embedded in WD-40. Other smaller crystals are also visible.

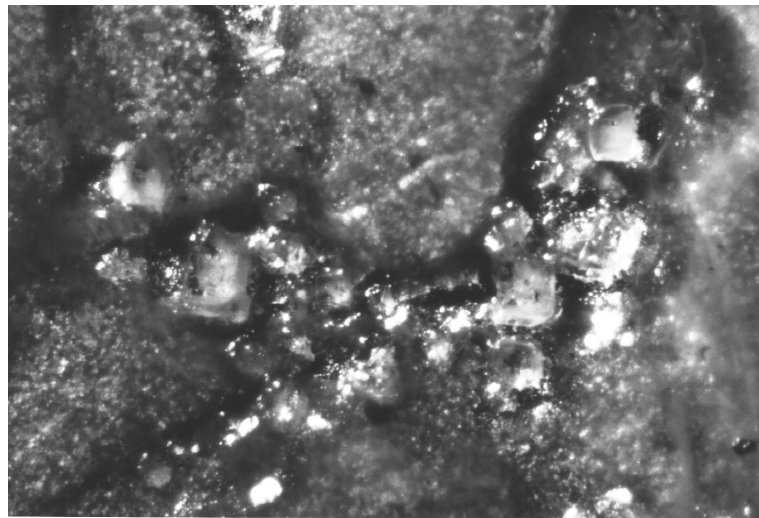


Figure 41. Group of crystals on the frit of the clay Experiment H-19. Several groups such as this one were discovered on the surface of the frit.

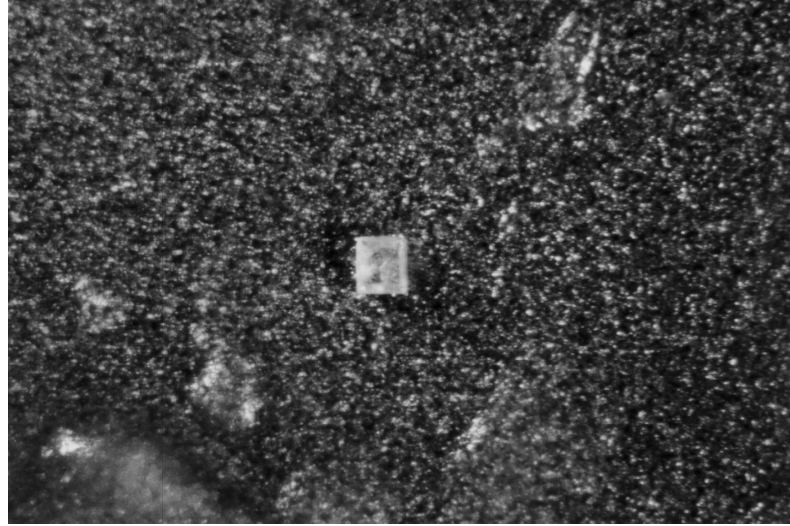


Figure 42. Crystal on the frit of the control (Experiment H-20). On the entire surface of the frit only two such crystals were found that were nearly identical in appearance. While the photographs do not show the frit to be totally devoid of crystals the contrast in number and appearance is dramatic.

Discussion

Before discussing the results, it is necessary to calculate the membrane coefficients for each of the experiments. Whitworth and DeRosa (1997) derived a steady-state solution for σ that does not use the measured values for c_e . This can be done, because at steady-state $c_e = c_i$. Therefore, by substituting Equation 4 into Equation 1 we obtain

$$J_v = L_p(\Delta P - \sigma v RT(c_o - c_e)) \quad (12)$$

which, since $c_e = c_i$ at steady-state, is the equivalent of

$$J_v = L_p(\Delta P - \sigma v RT(c_o - c_i)) \quad (13)$$

Fritz and Marine (1983) stated that

$$\omega = \frac{D}{RT\Delta x \zeta} \quad (14)$$

where ζ is the tortuosity of the flow path through the membrane defined by the ratio of the actual length divided by the membrane thickness. By substituting Equation 4, Equation 13, and the steady-state relationship $J_s = J_v c_e$ into Equation 2 we obtain

$$J_v \cdot c_i = \frac{c_o + c_i}{2} (1 - \sigma) J_v + \frac{D}{RT\Delta x \zeta} v RT (c_o - c_i) \quad (15)$$

Solving equations 12 and 14 for σ and setting them equal, we obtain

$$\frac{\frac{L_p \Delta P - J_v}{L_p v R T (c_o - c_i)}}{\frac{2 D v (c_o - c_i)}{\Delta x \zeta} - J_v (c_i - c_o)} = \frac{2 D v (c_o - c_i)}{\Delta x \zeta} - J_v (c_i - c_o) \quad (16)$$

Solving this equation for c_0 yields a polynomial solution with two roots, one positive and one negative root.

$$\text{root1} = \frac{1}{2 L_p v R T (J_v \Delta x - 2 v D)} \cdot (-2 L_p v R T J_v c_i \Delta x \zeta - 4 L_p v^2 R T D c_i + \Delta x \zeta J_v L_p \Delta P + \Delta x^{1/2} \zeta^{1/2} (-8 \zeta \Delta x c_i J_v^3 T R v L_p + 8 \zeta \Delta x c_i J_v^2 T R v L_p^2 + \zeta \Delta x J_v^4 - 2 \zeta \Delta x \Delta P L_p J_v^3 + \zeta \Delta x \Delta P^2 L_p^2 J_v^2 - 16 J_v^2 c_i D T R v^2 L_p^2)^{1/2}) \quad (17)$$

$$\text{root2} = \frac{1}{2 L_p v R T (J_v \Delta x - 2 v D)} \cdot (-2 L_p v R T J_v c_i \Delta x \zeta - 4 L_p v^2 R T D c_i + \Delta x \zeta J_v L_p \Delta P - \Delta x^{1/2} \zeta^{1/2} (-8 \zeta \Delta x c_i J_v^3 T R v L_p + 8 \zeta \Delta x c_i J_v^2 T R v L_p^2 + \zeta \Delta x J_v^4 - 2 \zeta \Delta x \Delta P L_p J_v^3 + \zeta \Delta x \Delta P^2 L_p^2 J_v^2 - 16 J_v^2 c_i D T R v^2 L_p^2)^{1/2}) \quad (18)$$

Since negative values of σ have no meaning, the positive root (root 2) is chosen to calculate c_o . The reflection coefficient is then calculated from

$$\sigma = \frac{-(J_v - L_p \Delta P)}{(L_p v R T c_o - L_p v R T c_i)} \quad (19)$$

The membrane coefficients σ , ω and c_o were calculated (Table 8) for each of the five experiments that used clay membranes using the approach of Whitworth and DeRosa (1997). Table 8 is a summary table and contains values of the measured experimental parameters as well as the calculated steady-state values of the membrane coefficients. The data in Table 8 is the basis for the discussion of the results that follows.

We see from Table 24 that when the calculated values of c_o are above solubility for NaCl (about 6.2M) that precipitation was observed. Experiment H-2 exhibited precipitation even though the calculated value of c_o was 6.11 molar, slightly below NaCl solubility. This precipitate may have been due to inadequate displacement of the brine from the cell by oil and subsequent evaporation.

Table 24. Experimental Results and Calculated Membrane Coefficients

Experiment	Δx (cm)	M_c (g)	Clay Type	ϕ (%)	Hydraulic Pressure (psi)	J_{vw} (cm/s) ($\times 10^{-4}$)	ΔP_w (psi)	J_v (cm/s) ($\times 10^{-4}$)	ΔP (PSI)	C_i (M)	C_o (M)	σ unitless	ω ($\times 10^{-15}$) (mole/dyne·s)	L_p ($\times 10^{-12}$) ($\text{cm}^3/\text{dyne}\cdot\text{s}$)	NaCl Precipitation Observed
H-1	0.0083	0.1392	B	32.2	30,000	0.159	1200	0.11	1203	4.56	--	--	--	0.19	Yes--Microprobe
H-2	0.0257	0.4985	K	30.5	50,000	18.6	600	10.95	543	4.64	6.11	0.18	3.5	45.6	Yes--Microprobe
H-3	0.0285	0.4999	K	37.1	50,000	10.8	700	9.86	1009	4.82	6.98	0.24	3.2	22.5	Yes--Microprobe
H-4	0.0095	0.1483	B	44.0	30,000	2.66	1000	1.64	795	4.90	5.52	0.40	9.5	3.85	No
H-19	0.0588	0.8702	K	90	50,000	8.22	640	0.515	810	4.72	6.46	0.62	1.5	18.6	Yes-abundant-microscope
H-20	NA	NA	NA	NA	NA	8.22	NA	NA	10	4.72	NA	NA	NA	NA	Yes-very sparse-Microscope

8

Note: M_c is mass of freeze-dried clay, K is kaolinite, B is bentonite, J_{vw} is flux of deionized water through membrane, ΔP_w is hydraulic pressure at steady state for run with deionized water. Values of σ , ω , and c_o are calculated using the method of Whitworth and DeRosa (1997). To convert psi to dynes/cm² multiply by 68947.57.

No calculated values of the membrane coefficients are shown for Experiment H-1 because the calculated values made no physical sense. This is attributed to a probable error in experimental measurement of L_p .

Much of the clay membrane literature implies that kaolinite, because it is essentially uncharged, is never as efficient a membrane as bentonite, montmorillonite, or smectite, all of which have significant negative charges on the crystalline lattice (Fritz and Marine 1983). Fritz (1986) states that most of the ion rejection capability of clays occurs because the negatively charged electrical field in the clay pore (the double layer) repels the anion. This is commonly called anion rejection. Surprisingly, hyperfiltration of undersaturated NaCl brine solutions through kaolinite resulted in more frequent NaCl precipitation than did hyperfiltration through bentonite. This suggests that, especially for concentrated solutions, that solute separation is most likely a function of the relative size of the solute and the pore size of the clay. The electric charge of the clay appears to be a secondary separation mechanism at best for brines. This is a reasonable and expected conclusion, because at concentrations above one molar, the electrical double layer is thought to collapse completely.

The results of these experiments suggest that hyperfiltration-induced solute precipitation is possible, even for very soluble substances such as NaCl. However, the precipitation rates do not appear to be adequate for commercial application at this time. Future experiments will focus on making the clay membranes more compact and thinner in order to obtain higher flux rates. Two alternative methods of removing solutes from solution, for which the New Mexico Tech Research Foundation is preparing patent applications, are also being investigated. These will be reported in the next annual report after the patent applications are filed.

Summary and Conclusions

Twenty different hyperfiltration-induced experiments were either attempted or completed and are reported here. The results of these experiments suggest that hyperfiltration-induced solute precipitation is possible, even for very soluble substances such as NaCl. However, the precipitation rates do not appear to be adequate for commercial application at this time. Future experiments will focus on making the clay membranes more compact and thinner in order to obtain higher flux rates. Two alternative methods of removing solutes from solution, for which the New Mexico Tech Research Foundation is preparing patent applications, are also being investigated. These methods will be described in the next annual report after the patent applications are filed.

TECHNOLOGY TRANSFER

On November 2-3, 2000, the kickoff meeting was held at the Merriot Courtyard Hotel, Farmington, New Mexico. Research members of this project were introduced to the participants. Besides John Ford, the NPTO/DOE project manager and eight research members, there were 12 industry representatives, 12 BLM representatives from the Colorado and New Mexico District Offices and Washington D.C. headquarter, two New Mexico Oil Conservation Division representatives, and one New Mexico State Representative. Members of the research team explained the main theory, the preliminary results and the goal of the proposed project. Del Fortner of BLM requested a side meeting, at which BLM agreed to support a proposed feasibility study for beneficial uses of produced water. The additional proposed study will compliment the existing effort. The study will be overseen by representatives from BLM, NMOCD, NPTO/DOE, NMOGA, and New Mexico Tech.

With input from the participants, an additional work plan was adopted by the research team. Currently, we are also gathering data on the chemistry and quantity of produced water from independent producers in San Juan Basin area. We will examine these analyses for potential treatment problems such as naturally occurring radioactive material (NORM) so that we can design our process for the actual water chemistry, and, importantly, choose representative samples of actual produced waters to use for bench-scale testing. So far we have gathered data from Bayless, Dugan Production, Cross Timber, and BLM-Colorado. The following entities have also agreed to provide produced water data: BLM-New Mexico, New Mexico OCD, Burlington, Devon, BP, Conoco, Texaco, and Phillips, Merrion. This data will also be made available on the WEB to interested parties (with permission of the providers).

The following account of the first annual project review is from the summer 2001 issue of *PRRC Review*, our division's biannual newsletter:

Producers, scientists, and members of the Lea County Water Users Association attended the project review of the NPTO/DOE-sponsored project, "Modified Reverse Osmosis System for Treatment of Produced Water," familiarly called the Waterdog project. This project aims to create a low-cost clay membrane for modified reverse osmosis treatment of produced water. The final waste stream is to be reduced to a solid for easy disposal. Through these studies, researchers foresee a low-cost, feasible treatment for produced oilfield waters, which are very high in salts and a headache to dispose of. The ultimate product will be a mobile unit small enough to be mounted in a trailer so it can treat water in remote locations.

The review was held June 26 at New Mexico Junior College in Hobbs, New Mexico. Morning speakers featured John Ford of the National Petroleum Technology Office of the Department of Energy, who introduced the project and spoke on NPTO efforts with produced water. He was followed by Lea County officials and industry experts who presented aspects of water quality issues.

Lea County Manager Dennis Holmberg introduced the Lea County Management Plan. He gave the overall picture of Lea County's efforts to develop and implement a 40-year water plan while protecting its nonreplenishable water supply.

Will Palmer of Read and Stevens spoke on development of a facility for Lea County capable of treating at least 150,000 bbl/d of produced water, converting it to usable water suitable for irrigation, recreation, and industrial use. Ken Marsh, an expert on oilfield-produced water, talked about water disposal methods. Finally, Eddie Livingston of Livingston Associates presented his company's successful pilot desalination plant in Alamogordo.

In the afternoon, Robert Lee, Project Manager, from the Petroleum Recovery Research Center at New Mexico Tech gave an overview of the Waterdog Project. Mike Whitworth, Principal Investigator, from the University of Missouri-Rolla discussed the advances the team has made over the past year, including:

- Construction of bench experimental apparatus
- Design, construction and testing of clay membranes
- Performance of dissolved solids precipitation experiments
- Progress on developing GIS produced water maps for San Juan and Permian Basins

The project team is also gathering data on the chemistry and quantity of produced water in the San Juan Basin area. Data analysis will allow researchers to design the experimental process for the actual water chemistry, and, importantly, to choose representative samples of actual produced waters to use for bench-scale testing.

Patent Number 6,241,892, "Method of Reducing the Contamination Level of a Solvent Purification System, and Such Solvent Purification System" issued May 2001 to the NMT Research Foundation. The inventor is T. M. Whitworth. Three additional patents resulting from this project are currently under development.

We are also compiling a list of potential beneficial uses of produced waters in the state of New Mexico. One graduate student, David Torres, is assigned to report on identifying beneficial uses and their water quality requirements.

Because of the research on this project T. M. (Mike) Whitworth was asked to sit on the advisory board for development of a new water treatment facility for the City of El Paso, Texas.

Presentations

- A talk by Robert Lee, "Modified Reverse Osmosis System for Treatment of Produced Water," was presented at the February 8, 2001⁸ SPE meeting at NMT, Socorro, NM.
- A talk by Bing Ye at PRRC Research Day, April 26, 2001, "Clay Membranes for Treatment of Produced Waters."
- A talk by David Torres Research Day, April 26, 2001, "Precipitation of NaCl using Clay Membranes."
- Mike Whitworth and Robert L. Lee, Presentation May 17, Livingston Associates, Alamogordo, New Mexico. Contact: Eddie Livingston (505-439-8588), who is in charge of Tularosa basin water project for City of Alamogordo.
- Mike Whitworth & Robert L. Lee, Presentation, May 18, El Paso Water Utilities (EPWU), El Paso, Texas. Contact: John Balliew (915-594-5595), who is in charge of the Desalination project for EPWU.

Peer-Reviewed Publications

- Whitworth, T. M., and Gu, Chen, 2001, Hyperfiltration-Induced Precipitation of Sodium Chloride, New Mexico Water Resources Research Institute Technical Completion Report No. 314, Las Cruces, New Mexico, 39 p
- Several papers are being prepared for submission to journals based on data presented in this report.

SUMMARY AND CONCLUSIONS

This report describes work performed during the first year of the project "Modified reverse osmosis system for treatment of produced waters." This research project has two objectives. The first objective is to test the use of clay membranes in reverse osmosis treatment of produced waters. The second objective is to test the ability of a system patented by the New Mexico Tech Research Foundation to remove salts from reverse osmosis waste streams as a solid. We performed 12 experiments using clay membranes in cross-flow reverse osmosis experimental cells. We found that, due to dispersion in the porous frit used adjacent to the membrane, the concentration polarization layer seems to be completely (or nearly completely) destroyed at low flow rates. This observation suggests that clay membranes used with porous frit material may reach optimum rejection rates at lower pumping rates than those required for use with synthetic membranes. The solute rejection efficiency in the cross-flow configuration decreases with increasing solution concentration. For the membranes and experiments reported here, the rejection efficiency ranged from 71% with 0.01 M NaCl solution down to 12 % with 2.3 M NaCl solution. The clay membranes used in our experiments were relatively thick (approximately 0.5 mm). The active layer of most synthetic membranes is only 0.04 μm (0.00004 mm), approximately 1250 times thinner than the clay membranes used in these experiments. Yet clay membranes as this as 12 μm have been constructed (Fritz and Eady, 1985). Since Darcy's law states that the flow through a material of constant permeability is inversely proportional to its thickness, then, based on these experimental observations, a very thin clay membrane would be expected to have much higher flow rates than the ones used in these experiments. Future experiments will focus on testing very thin clay membranes. The membranes generally exhibited stable rejection rates over time for chloride for a range of concentrations between 0.01 and 2.5 M. One membrane ran in excess of three months with no apparent loss of usability. This suggests that clay membranes may have a long useable life.

Twenty different hyperfiltration-induced solute precipitation experiments were either attempted or completed and are reported here. The results of these experiments suggest that hyperfiltration-induced solute precipitation is possible, even for very soluble substances such as NaCl. However, the precipitation rates achieved in our laboratory do not appear to be adequate for commercial application at this time. Future experiments will focus on making the clay membranes more compact and thinner in order to obtain higher flux rates. Two alternative methods of removing solutes from solution for which the New Mexico Tech Research Foundation is preparing patent applications are also being investigated. These methods will be described in the next annual report after the patent applications are filed.

Technology transfer efforts included two meetings (one in Farmington NM, and one in Hobbs, NM) where the results of this research were presented to independent oil producers and other interested parties. In addition, members of the research team gave eight presentations concerning this research and because of the research on this project T. M. (Mike) Whitworth was asked to sit on the advisory board for development of a new water treatment facility for the City of El Paso, Texas. Several papers are in preparation for submission to peer-reviewed journals based on the data presented in this report.

REFERENCES CITED

Barone, F. S.; Rowe, R. K.; and Quigley, R. M., 1992. Estimation of chloride diffusion coefficient and tortuosity factor for mudstone: *Journal of Geotechnical Engineering*. v. 118, p. 1031-1047.

Barone, F. S.; Rowe, R. K.; and Quigley, R. M., 1990. Laboratory determination of chloride diffusion coefficient in intact shale: *Canadian Geotechnical Journal*. v. 27, p. 177-184.

Benzel, W. M. and Graf, D. L., 1984. Studies of smectite membrane behavior: Importance of layer thickness and fabric in experiments at 20°C, *Geochimica et Cosmochimica Acta*, 48: 1769-1778.

Campbell, D. J., 1985. Fractionation of stable chlorine isotopes during transport through semipermeable membranes. M.S. thesis, University of Arizona, 103 p.

Coplen, T. B., and Hanshaw, B. B., 1973. Ultrafiltration by a compacted membrane--I. Oxygen and hydrogen isotope fractionation., *Geochimica et Cosmochimica Acta*, 37: 2205-2310.

Cox, D. O.; Decker, A. D.; and Stevens, S. H., 1993. Analysis of fruitland water production treatment and disposal: San Juan Basin, Topical Report GRI-93/0288, Gas Research Institute, 333 p.

Demir, I., 1988. Studies of smectite membrane behavior: Electrokinetic, osmotic, and isotopic fractionation processes at elevated pressures. *Geochimica et Cosmochimica Acta*, 52: 727-737.

Elrick, D. E., Smiles, D. E., Baumgartner, N., and Groenveld, P. H., 1976, Coupling phenomena in saturated homo-ionic montmorillonite: I. *Experimental, Soil Science Society of America Journal*, v. 40, 490-491.

Feth, J. H., 1970. Saline groundwater resources of the conterminous United States. *Water Resources Research*, 6: 1454-1457.

Fritz, S. J. 1986. Ideality of clay membranes in osmotic processes: a review. *Clays and Clay Minerals*. 34: 214-223.

Fritz, S. J. and C. D. Eady, 1985. Hyperfiltration-induced precipitation of calcite. *Geochimica et Cosmochimica Acta*. 49: 761-768.

Fritz, S.J. and Marine, I.W., 1983. Experimental support for a predictive osmotic model of clay membranes: *Geochimica et Cosmochimica Acta*, 47: 1515-1522.

Fritz, S. J., Hinz, D. L., and Grossman, E. L., 1987. Hyperfiltration-induced fractionation of carbon isotopes, *Geochemica et Cosmochimica Acta* , 51: 1121-1134, .

Fritz, S. J. and Whitworth, T. M., 1994. Hyperfiltration-induced fractionation of lithium isotopes: ramifications relating to representativeness of aquifer sampling. *Water Resources Research*, 30: 225-235.

Harris, F. L., Humphreys, G. B., and Spiegler, K. S., 1976. Reverse osmosis (hyperfiltration) in water desalination, in P. Meares, ed., *Membrane Separation Processes*, Elsevier, Amsterdam, Chapter 4.

Haydon, P. R., and Graf, D. L., 1986. Studies of smectite membrane behavior: Temperature dependence, 20-180°C, *Geochemica et Cosmochimica Acta* , 50: 115-121.

Hirschfeld, D. A., Li, T. K. and Liu, D. M.. 1996, Processing of porous oxide ceramics, in. *Porous Ceramic Materials*, Liu, D-M, Editor, Trans Tech Publications, pp.65-80.

Ishiguro, M., Matsuura, T. and Detellier, C., 1995. Reverse osmosis separation for a montmorillonite membrane, *Journal of Membrane Science*, 107: 87-92.

Kedem, O. and Katchalsky, A. 1962. A physical interpretation of the phenomenological coefficients of membrane permeability, *Journal of General Physiology*. 45: 143-179.

Kemper, W. D., 1961. Movement of water as effected by free energy and pressure gradients. I. Application of classic equations for viscous and diffusive movements to the liquid phase in finely porous media. II. Experimental analysis of porous systems in which free energy and pressure gradients act in opposite directions, *Proc. Soil Sci. America*, 25: 255-265.

Kemper, W. D., 1960. Water and ion movement in thin films as influenced by the electrostatic charge and diffuse layer of cations associated with clay mineral surfaces, *Proc. Soil Sci. America*, p. 10-16.

Kemper, W. D. and Rollins, J. B., 1966. Osmotic efficiency coefficients across compacted clays, *Proc. Soil Sci. America*, 30: 529-534.

Kharaka, Y. K. and Smalley, W. C., 1976. Flow of water and solutes through compacted clays. *American Assoc. Pet. Geol. Bull.*, 60: 973-980.

Kharaka, Y. K. and Berry, F. A. F., 1973. Simultaneous flow of water and solutes through geologic membranes, I. Experimental investigation, *Geochimica et Cosmochimica Acta*, 37: 2577-2603.

Mariñas, B. J. and Selleck, R. E., 1992, Reverse Osmosis treatment of multicomponent electrolyte solutions, *Journal of Membrane Science*, v. 72, p. 211-229.

Marine, I. W., and Fritz, S. J., 1981. Osmotic model to explain anomalous hydraulic heads, *Water Resources Research*, 17: 73-82.

Mitsoyannis, E. and Saravacos, G. D., 1977, Precipitation of calcium carbonate on reverse osmosis membranes, *Desalination*, v. 21, 235-240.

Montgomery, James Consulting Engineers, Inc, 1985. *Water treatment principles and design*, John Wiley & Sons, New York, 696 p.

Olsen, H. W., 1972. Liquid movement through kaolinite under hydraulic, electric, and osmotic gradients, *American Association of Petroleum Geologists Bulletin*, 56: 2022-2028.

Olsen, H. W., 1969. Simultaneous fluxes of liquid and charge in saturated kaolinite, *Proc. Soil Sci. America*, 33: 338-344.

Spiegler, K. S. and Kedem, O., 1966, Thermodynamics of hyperfiltration (reverse osmosis): criteria for efficient membranes, *Desalination*, v 1, p. 311-326.

Srivastava, R. C. and Jain, A. K., 1975. Non-equilibrium thermodynamics of electro-osmosis of water through composite clay membranes, 1. The electro-kinetic energy conversion, *Journal of Hydrology*, 25: 307-324.

Tait, J. H. and Brandt, H., 1992. Process for coal-bed methane brine disposal, *American Oil and Gas Reporter*, Sept.

Whitworth, T. M., and Gu, Chen, 2001, Hyperfiltration-induced precipitation of sodium chloride, New Mexico Water Resources Research Institute Technical Completion Report No. 314, Las Cruces, New Mexico, 39 p.

Whitworth, T. M., 1999, Clay Minerals—Ion Exchange. In *The Encyclopedia of Geochemistry*, Fairbridge, R. W. and Marshall, C. P., eds., Chapman and Hall (invited), pp. 85-87.

Whitworth, T. M. and DeRosa, G., 1997. Geologic membrane controls on saturated zone heavy metal transport. New Mexico Water Resources Research Institute Report No. 303, Las Cruces, New Mexico, 88 p.

Whitworth, T. M., Marinas, B. J., and Fritz, S. J., 1994, Isotopic fractionation and overall permeation of lithium by a thin-film polyamide reverse osmosis membrane. *Journal of Membrane Science*, v. 88, pp. 231-241.

Whitworth, T. M. and Fritz, S. J., 1994. Interrelationship between solute-induced permeability increase and membrane effect in clays. *Applied Geochemistry*, 9: 533-546.

Wyllie, M. R. J., 1948. Some electrochemical properties of shales, *Science*, 108: 684-685.

Wyllie, M. R. J., 1949. A quantitative analysis of the electrochemical component of the S. P. curve, *J. Petroleum Tech.*, 1: 17-26.

Zimpfer, G; Harmon, E.; and Boyce, B., 1988. Disposal of production waters from oil and gas wells in the Northern San Juan Basin, Colorado, in Fassett, J., ed., *Geology and Coal-bed methane resources of the northern San Juan Basin, Colorado and New Mexico*, Rocky Mountain Association of Geologists, pp. 183-198.

Zimmie, T. F. and Almaleh, L. J., 1975, Shrinkage of soil specimens during preparation for porosimetry tests. p. 202-215. in: *Soil Specimen Preparation for Laboratory Testing*. American Society for Testing and Materials special technical publication 599, 340 p.

APPENDIX A: Chemical Analysis for Waterdog Project

Table A-1 summarizes the methods used for the chemical analyses presented in this report. Ion Chromatography (IC) was used for low concentrations of chloride (below 200 ppm) and for sulfate analysis. The ion chromatograph used was a Dionex 600 with an AS50 autosampler and chromatography compartment, a CD25 conductivity detector and a GP50 gradient pump. The column used was a Dionex AS14. Calibration was done by injecting a series of standard solutions. Low concentration of chloride and sulfate were analyzed by using the Dionex 600 with an AS50 autosampler and chromatography compartment, CD25 conductivity detector and a GP50 gradient pump. The column used is AS14.

Internal reference standards are run near the beginning and end of each IC run. Occasionally, calibration checks are run every 20-30 samples if it is a large run. If it is known that some samples will have particularly high concentration, a blank is run after these samples. A duplicate sample was run every 10-12 samples. Internal reference standards of Cl = 40.5 SO₄ = 91.5 were periodically run. The results of these analyses were Cl = 40.5, 40.6, 40.2 and SO₄ = 92.4, 92.3, 92.7.

Table A-1. Summary of Analytical Methods, Accuracy, and Precision for Chemical Analyses

Species	Equipment	Method Number	Accuracy	Precision
Chloride (<200ppm)	IC	EPA300.0	< 1%	< 0.5%
Sulfate	IC	EPA300.0	< 1%	< 0.5%
Sodium	FAA	EPA7000	2%	1%
Potassium	FAA	EPA7000	3%	1%
Calcium	FAA	EPA7000	2%	1%
Magnesium	FAA	EPA7000	2%	1%
Chloride (>200ppm)	FIA	QuikChem 10-117-07-1-J	0.5%	0.5%

Note: Accuracy and precision are stated at one standard deviation.

High chloride concentrations (above 200 ppm) were analyzed by using a Lachat Quik-Chem 8000® flow injection analysis automated ion analyzer (FIA) made by Zellweger Analytics, INC. This system consists of the following modules: a QuikChem FIA⁺ System Unit, a Dual Resolution Dilutor (DRD), and a Cetac ASX-500 Autosampler. The system is computer controlled using the Omnitron FIA data acquisition program. The method used was QuikChem Method 10-117-07-1-J. This method covers the determination of chloride in drinking, ground, and surface waters, and domestic and industrial wastes. The applicable range is 200 to 25,000 mg Cl/L. The method detection limit is 7.3 mg Cl/L. Dilutions were made when concentrations were above this range.

A stock solution of 25,000 mg Cl/L was freshly made by dissolving primary standard grade sodium chloride (NaCl) in Deionized water (10 megohm). The sodium chloride was dried in a 105°C oven overnight and then weighted to the nearest 0.0001g. All the other standard solutions such as 12,500, 6250, 3125, and 1000 mg Cl/L were made by diluting different volume of stock solution in a volumetric flask.

Calibration was done by injecting a series of standard solutions. Triplicate analysis were conducted for each standard solution and a 0.5% RSD was set as replicate criteria. The data system will then prepare a calibration curve by plotting responses versus standard concentrations.

The calibration was a third-order polynomial curve. Sample concentration was calculated from the regression equation. During sample analysis procedures, the Data Quality Management (DQM) plan was activated by analyzing the blank and middle range standard solution after every 10-sample analysis. Again, 0.5% RSD was set as a criterion. If the criterion was not satisfied, the calibration curve was reestablished. For samples whose concentrations were out of the range of calibration standard, the autodilution function was triggered and the samples were reanalyzed.

Cation analysis was conducted by using Varian Model 110 Flame Atomic Absorption (FAA), SIPS-10 Sample Introduction Pump System, and SPS-5 Sample Preparation System and Dilutor. Calibration check samples were run at the beginning and end of each run, and after every 10–12 samples if there were more than 20 samples in a run. A duplicate sample was run every for 10–12 samples. The instrument was checked for zero readings between samples and re-zeroed if necessary, re-sloped every 10–12 samples and re-calibrated every 20–24 samples.